CSIAM Trans. Life Sci.
doi: 10.4208/csiam-ls.SO-2025-0006

Vol. **x**, No. x, pp. 1-34
xx 2025

Stochastic Dynamics Between HIV-1 Latent Infection and cART Efficacy Within the Brain Microenvironment

Yiping Tan[1], Suli Liu[2], Yongli Cai[3], Xiaodan Sun[4], Zhihang Peng[5,*] and Weiming Wang[6,*]

[1] *School of Mathematics and Statistics, Huaiyin Normal University, Huaian 223300, China.*
[2] *School of Mathematics, Jilin University, Changchun 130012, China.*
[3] *School of Mathematics and Statistics, Nantong University, Nantong 226019, China.*
[4] *School of Mathematics and Statistics, Xi'an Jiaotong University, Xi'an 710049, China.*
[5] *National Key Laboratory of Intelligent Tracking and Forecasting for Infectious Diseases, Chinese Center for Disease Control and Prevention, Beijing 102206, China.*
[6] *School of Computer Science and Technology, Huaiyin Normal University, Huaian 223300, China.*

Received 15 April 2025; Accepted 21 July 2025

The authors sincerely congratulate Prof. Zhien Ma on his 90th birthday and to celebrate his long-lasting impact on the field of mathematical biology and differential equations.

Abstract. We develop a stochastic human immunodeficiency virus type 1 (HIV-1) infection model to analyze combination antiretroviral therapy (cART) dynamics in the brain microenvironment, explicitly accounting for two infected cell states: (1) productively infected and (2) latently infected populations. The model introduces two key epidemiological thresholds – $\overline{\mathcal{R}}_{c1}$ (productive infection) and $\overline{\mathcal{R}}_{c2}$ (latent infection) – and defines the stochastic control reproduction number as $\overline{\mathcal{R}}_c = \max\{\overline{\mathcal{R}}_{c1}, \overline{\mathcal{R}}_{c2}\}$. Our analysis reveals three distinct dynamical regimes: (1) viral extinction ($\overline{\mathcal{R}}_c < 1$): the infection clears exponentially with probability one; (2) latent reservoir dominance ($\overline{\mathcal{R}}_c = \overline{\mathcal{R}}_{c2} > 1$): the system almost surely converges to a purely latent state, characterizing stable viral reservoir formation; (3) persistent productive infection ($\overline{\mathcal{R}}_c = \overline{\mathcal{R}}_{c1} > 1$): the infection persists indefinitely with a unique stationary distribution, for which we derive the exact probability density function. And numerical simulations validate these theoretical predictions, demonstrating how environmental noise critically modulates HIV-1 dynamics in neural reservoirs. Our results quantify the stochastic balance between productive infection, latency establishment, and cART efficacy, offering mechanistic insights into viral persistence in the brain.

*Corresponding author. *Email addresses:* zhihangpeng@njmu.edu.cn (Z. Peng), wangwm_math@hytc.edu.cn (W. Wang)

AMS subject classifications: 60H10, 60H25, 92D30, 39A50

Key words: Brain reservoirs, combination antiretroviral therapy, HIV-1 infection model, extinction, probability density function.

1 Introduction

The brain serves as a major reservoir for human immunodeficiency virus type 1, harboring populations of long-lived infected brain macrophages that contribute to the persistence of viral infection and pose significant challenges for viral eradication [36]. Substantial evidence indicates that HIV-1 crosses the blood-brain barrier (BBB) through either free viral particles or infected macrophages, establishing cerebral infection within two weeks of initial exposure [29]. Within the central nervous system (CNS), viral infection primarily targets long-lived myeloid cells, including perivascular macrophages, microglia, and astrocytes [33,34]. Current clinical management relies on combination antiretroviral therapy (cART) to suppress viral load, slow disease progression, and reduce the size of latent viral reservoirs [5, 8, 37].

However, the efficacy of cART in the brain is significantly constrained by two major factors: (1) BBB restricts drug penetration, and (2) diminished immune surveillance creates a potential viral sanctuary [36,51]. Both experimental and clinical studies demonstrate that while cART effectively suppresses HIV-1 RNA production, it shows limited impact on viral DNA levels within the brain [22, 38, 59]. This suggests that cART primarily targets productive infection while failing to eliminate latent viral reservoirs.

Latently infected cells are currently defined as cells harboring integrated, intact proviruses capable of reversible viral production arrest [18, 34]. However, this definition remains largely theoretical. To date, only resting CD4+ T cells fully satisfy this criterion, while the virological characteristics of other cell types require further validation [18, 19, 50]. Notably, cells of the monocyte/macrophage lineage exhibit distinct behavior – they maintain low-level viral replication rather than complete transcriptional silence [19, 50]. Emerging evidence indicates that latently infected brain macrophages may retain minimal but detectable infectivity, distinguishing them from truly healthy cells [25, 28, 41].

Recent experimental evidence demonstrates that HIV-1-infected macrophages/microglia can survive acute infection and establish latent infection by 21 days post-infection, with retained capacity for viral reactivation [10]. A dynamic equilibrium exists between productively and latently infected brain macrophages, characterized by continuous stochastic transitions between activated and deactivated states [10, 20, 36, 51]. While cART exhibits variable penetration efficacy in brain macrophages and tissues [2, 10], it effectively reduces both cerebrospinal fluid (CSF) viral load and cerebral viral RNA levels [59]. This reduction likely reflects decreased populations of activated brain macrophages [21], suggesting that cART may significantly alter the baseline equilibrium between activation states, favoring deactivation [24, 41]. Conversely, latency reversing agents (LRAs)

appear to shift this equilibrium toward activation [55]. Notably, latently infected brain macrophages represent a persistent reservoir capable of viral reactivation, potentially explaining the rapid plasma viral rebound observed following cART interruption [36, 50].

HIV-associated neurocognitive disorder (HAND) remains a significant clinical challenge in HIV-1 infection, characterized by varying degrees of cognitive impairment in affected patients [12]. Although the precise pathogenic mechanisms of HAND remain incompletely understood, current evidence strongly implicates brain macrophage infection and viral load levels as key determinants of disease severity. Supporting this notion, recent simian immunodeficiency virus (SIV) infection models have demonstrated a direct correlation between higher viral loads and more severe neurocognitive impairment [20, 32]. While cART has demonstrated efficacy in ameliorating neurological symptoms, particularly in cases of HIV-associated dementia, treated patients continue to exhibit suboptimal performance on standardized neurocognitive assessments [47]. Notably, milder forms of HAND maintain a concerning prevalence of approximately 42.6% among treated individuals [52]. From a clinical perspective, preventing neurological complications represents a critical priority for improving quality of life in people living with HIV-1. Compared to the formidable challenge of achieving complete viral eradication – which remains a distant goal – neurological protection offers a more immediate and achievable therapeutic target for this patient population [32].

The brain microenvironment introduces multiple stochastic factors influencing HIV-1 dynamics, including: (1) temporal variations in immune surveillance efficiency, (2) stochastic reactivation of latently infected cells, and (3) probabilistic transmigration of viral particles and infected cells across the BBB [13, 17, 42]. Notably, both HIV-1 and infected macrophages have been shown to breach the BBB and establish cerebral infection during early stages of systemic infection [6]. Of particular clinical relevance is the observation that upon cessation of cART, CNS-resident viral populations can reseed peripheral compartments, precipitating systemic viral rebound. This reservoir dynamics exhibits marked stochasticity, representing a fundamental mechanism underlying viral persistence and therapeutic failure [44]. Consequently, systematic investigation of HIV-1 infection dynamics incorporating environmental noise (i.e. extrinsic biological and physiological variability affecting macrophage dynamic behavior) represents a crucial research direction for understanding viral persistence and improving therapeutic outcomes.

Moreover, studies on complex dynamical systems in viral infections-particularly transmission processes-have consistently demonstrated that stochastic perturbations influence critical thresholds determining viral extinction or persistence [26, 27, 45, 53, 56]. Specifically, Wang *et al.* [54] analyzed stochastic HIV dynamics incorporating latent infection and cell-to-cell transmission, revealing that environmental fluctuations can promote viral clearance. Dalal *et al.* [16] developed a stochastic model of HIV-1 pathogenesis, showing that highly active antiretroviral therapy (HAART) can partially mitigate or even reverse disease progression. Recent work has further elucidated noise-dependent viral behavior through stationary distribution and probability density function analyses, providing deeper insights into stochastic influences on infection dynamics [46, 48].

There naturally comes a question: How do stochastic perturbations influence the dynamic interplay between HIV-1 latent infection and cART efficacy within the brain microenvironment?

The remainder of this paper is organized as follows. In Section 2, we formulate an HIV-1 latent infection model incorporating environmental noises. In Section 3, we give the stochastic dynamics of the model involving the stochastic extinction, the stationary distribution and probability density function. In Section 4, some numerical examples are performed to demonstrate the theoretical results and reveal the impact of environmental white noises. Finally, in Section 5, we end our work with some concluding remarks.

2 Model formulation

In order to eliminate the infection and minimize HAND by the most widely used cART along with efforts to optimize other treatment therapies in the brain, we need to fully understand the latent infection mechanism and the related HAND in the CNS under cART at first. Mathematical modelling is an effective and low-cost method to both qualitative and quantitative approaches this question, we recommend the representative references [40, 41].

In [41], the authors subdivided the brain macrophage into susceptible x, productively infected y, latent infected l, and the brain macrophages are described by the following differential equation in the absence of infection: $\mathrm{d}x/\mathrm{d}t = \lambda - kx$, where λ is the source of new susceptible brain macrophages and k is the death rate of brain macrophages. Based on the research evidence, they assumed that HIV-1 spreads principally by cell-to-cell transmission in the brain, HIV-1 related death rates of productively and latently infected macrophages are negligible. They assumed that both productively and latently infected macrophages have infectivity, even though the infectivity of latently infected macrophages could be at a very low level, and the infectious interaction is measured by the mass action terms $\beta_1 xy$ and $\beta_2 xl$. The action of cART ($0 \leq \epsilon \leq 1$ denotes the effectiveness) in the brain can be roughly divided into two aspects: reduce the infection rate of productively infected macrophages to $(1-\epsilon)\beta_1$ and deactivate productively infected macrophages to latent infected ones at the rate $\epsilon\gamma$. They assumed that the majority of newly infected macrophages will enter the latently infected population, only a fraction $p(1-\epsilon)\beta_1 xy$ will enter the productively infected macrophages. And the authors constructed an HIV-1 latent infection model described by the set of ordinary differential equations (ODEs) [41]

$$\begin{cases} \dfrac{\mathrm{d}x(t)}{\mathrm{d}t} = \lambda - kx(t) - (1-\epsilon)\beta_1 x(t)y(t) - \beta_2 x(t)l(t), \\ \dfrac{\mathrm{d}y(t)}{\mathrm{d}t} = p(1-\epsilon)\beta_1 x(t)y(t) - ky(t) - \epsilon\gamma y(t), \\ \dfrac{\mathrm{d}l(t)}{\mathrm{d}t} = (1-p)(1-\epsilon)\beta_1 x(t)y(t) + \beta_2 x(t)l(t) - kl(t) + \epsilon\gamma y(t), \end{cases} \tag{2.1}$$

Table 1: The meanings of the parameters of model (2.1).

Paras	Meanings	Unit
λ	Recruitment rate of susceptible macrophages	per g
β_1	Transmission rate between susceptible and productively infected macrophages	per year
β_2	Transmission rate between susceptible and latently infected macrophages	per year
k	Natural death rate of brain macrophages	per year
ϵ	Percentage of cART effectiveness and $\epsilon\in[0,1]$	unit-free
γ	Deactivated rate	per year
p	Proportion of newly infected macrophages and $p\in(0,1)$	unit-free
x_0	Initial value for x	per g
y_0	Initial value for y	per g
l_0	Initial value for l	per g

the biological meanings of the parameters of model (2.1) are shown in Table 1. This mathematical model effectively describes the biological phenomena of interest (as observed in clinical and experimental studies): the suppression of productively infected brain macrophages and the establishing of a latent reservoir of brain macrophages under cART.

After defining the control reproduction number

$$\mathcal{R}_c=\max\{\mathcal{R}_{c1},\mathcal{R}_{c2}\},$$

where

$$\mathcal{R}_{c1}=\frac{p(1-\epsilon)\beta_1\lambda}{k(k+\epsilon\gamma)},\quad \mathcal{R}_{c2}=\frac{\beta_2\lambda}{k^2},$$

the authors obtained the main dynamical results as follows:

(1) If $0<\mathcal{R}_c<1$ holds, the infection-free equilibrium $P_0=(\lambda/k,0,0)$ is globally asymptotically stable.

(2) If $\mathcal{R}_c>1$ and $\mathcal{R}_{c2}<\mathcal{R}_{c1}$ hold, the productive equilibrium $P_1=(x_1,y_1,l_1)$ is globally asymptotically stable, where

$$\begin{aligned}
x_1&=\frac{k+\epsilon\gamma}{p\beta_1(1-\epsilon)},\\
y_1&=\frac{\big(\lambda p(1-\epsilon)\beta_1-k(k+\epsilon\gamma)\big)\big(p(1-\epsilon)\beta_1k-\beta_2(k+\epsilon\gamma)\big)}{p(1-\epsilon)\beta_1k(k+\epsilon\gamma)\big((1-\epsilon)\beta_1-\beta_2\big)},\\
l_1&=\frac{\big((1-p)k+\epsilon\gamma\big)\big(\lambda p(1-\epsilon)\beta_1-k(k+\epsilon\gamma)\big)}{pk(k+\epsilon\gamma)\big((1-\epsilon)\beta_1-\beta_2\big)}.
\end{aligned}$$

(3) If $\mathcal{R}_c>1$ and $\mathcal{R}_{c1}<\mathcal{R}_{c2}$ hold, the latent equilibrium $P_2=(x_2,0,l_2)$ is globally asymptotically stable, where $x_2=k/\beta_2$ and $l_2=\lambda/k-k/\beta_2$.

It is worthy to note that, if $\beta_2 = 0$ in model (2.1), there is no latent equilibrium and the dynamics will be simplified as the classical threshold dichotomy like [14, 40]. And it is this latent equilibrium that allows model (2.1) to effectively describe the biological phenomena of interest. Model (2.1) was also used to simulate the effect of LRAs and show the effectiveness of "Shock and Kill" strategy numerically.

Building upon our analysis of environmental noise effects in the Section 1, we incorporate stochastic perturbations into the system through white noise terms that scale linearly with the state variables $x(t), y(t), l(t)$, and these noise terms directly modulate the temporal dynamics of each population, appearing as multiplicative components in the time derivatives $\mathrm{d}x(t)/\mathrm{d}t, \mathrm{d}y(t)/\mathrm{d}t, \mathrm{d}l(t)/\mathrm{d}t$, respectively. Specifically,

- $\sigma_1 x(t)\mathrm{d}B_1(t)$ captures the stochastic fluctuations in the number of healthy brain macrophages, arising from intrinsic variability in cell proliferation and immune responses, as well as external environmental disturbances;
- $\sigma_2 y(t)\mathrm{d}B_2(t)$ accounts for the random fluctuations in the productively infected brain macrophages, influenced by uncertainties in viral replication efficiency, immune clearance, and variability in cART penetration;
- $\sigma_3 l(t)\mathrm{d}B_3(t)$ reflects the stochastic reactivation and turnover of latently infected macrophages, as well as the probabilistic nature of drug efficacy in targeting the latent reservoir.

This formulation yields the following stochastic differential equation (SDE) system, which generalizes the deterministic ODE model (2.1):

$$\begin{cases} \mathrm{d}x(t) = \big(\lambda - kx(t) - (1-\epsilon)\beta_1 x(t)y(t) - \beta_2 x(t)l(t)\big)\mathrm{d}t + \sigma_1 x(t)\mathrm{d}B_1(t), & \text{(2.2a)} \\ \mathrm{d}y(t) = \big(p(1-\epsilon)\beta_1 x(t)y(t) - ky(t) - \epsilon\gamma y(t)\big)\mathrm{d}t + \sigma_2 y(t)\mathrm{d}B_2(t), & \text{(2.2b)} \\ \mathrm{d}l(t) = \big((1-p)(1-\epsilon)\beta_1 x(t)y(t) + \beta_2 x(t)l(t) - kl(t) + \epsilon\gamma y(t)\big)\mathrm{d}t + \sigma_3 l(t)\mathrm{d}B_3(t), & \text{(2.2c)} \end{cases}$$

where $\sigma_i\,(i=1,2,3)$ represent the intensities of the white noises, $B_i(t)\,(i=1,2,3)$ are mutually independent standard Brownian motions defined on the complete probability space $(\Omega, \mathcal{F}, \{\mathcal{F}_t\}_{t\geq 0}, \mathbb{P})$ with the filtration $\{\mathcal{F}_t\}_{t\geq 0}$ satisfying the usual condition, i.e. it is increasing and right continuous while $\mathcal{F}_0$ contains all $\mathbb{P}$-null sets.

It is widely accepted that macrophages are among the first cells targeted by HIV-1 [18, 50, 51]. In primates infected with a simian/human immunodeficiency virus (SHIV), exceed 95% of infected cells are tissue macrophages in the late stage of disease, and high viral loads in plasma produced by tissue macrophages can be seen after CD4+ T-cell depletion [7]. These indicate the significance of investigating the macrophages' infectious interaction. The model developed here and its mathematical results can be applied to monocyte/macrophage lineage cells of other tissues.

3 Stochastic dynamics of HIV-1 infection in brain macrophages

Firstly, we give the following theorem about the existence and uniqueness of the global positive solution of model (2.2).

Theorem 3.1. *For model* (2.2) *with any initial value* $(x(0),y(0),l(0))\in\mathbb{R}^3_+$*, there exists a unique global positive solution* $(x(t),y(t),l(t))$ *for* $t\geq 0$*, and the solution will remain in* $\mathbb{R}^3_+$ *with probability one.*

The proof is standard, and we refer the reader to [11, 39].

3.1 Stochastic extinction of HIV-1 infection

One of the most significant questions in viral dynamics is under what conditions the infection may be eliminated in a long term. Thus, we devote to investigate the stochastic extinction of the infection in this subsection.

Define

$$\overline{\mathcal{R}}_c := \max\{\overline{\mathcal{R}}_{c1},\overline{\mathcal{R}}_{c2}\}, \tag{3.1}$$

where

$$\overline{\mathcal{R}}_{c1}=\frac{p(1-\epsilon)\beta_1\lambda}{k\big(k+\epsilon\gamma+\sigma_2^2/2\big)},\quad \overline{\mathcal{R}}_{c2}=\frac{\beta_2\lambda}{k\big(k+\sigma_3^2/2\big)}. \tag{3.2}$$

Theorem 3.2. *Assume* $k>(\sigma_1^2\vee\sigma_2^2\vee\sigma_3^2)/2$*. Let* $(x(t),y(t),l(t))$ *be the solution of model* (2.2) *with the initial condition* $(x(0),y(0),l(0))\in\mathbb{R}^3_+$*, if* $\overline{\mathcal{R}}_c<1$*, then*

$$\lim_{t\to\infty}\frac{1}{t}\int_0^t x(s)\mathrm{d}s=\frac{\lambda}{k},\quad \limsup_{t\to\infty}\frac{\ln y(t)}{t}<0,\quad \limsup_{t\to\infty}\frac{\ln l(t)}{t}<0\quad a.s.$$

Namely, both productively and latently infected brain macrophages are eliminated with probability one.

Proof. Since the solution of model (2.2) is positive by Theorem 3.1, we have

$$\mathrm{d}x\leq(\lambda-kx)\mathrm{d}t+\sigma_1 x\mathrm{d}B_1(t).$$

Consider the following auxiliary stochastic differential equation:

$$\mathrm{d}T=(\lambda-kT)\mathrm{d}t+\sigma_1 T\mathrm{d}B_1(t)$$

with the initial value $T(0)=x(0)>0$. Then we can obtain

$$\lim_{t\to\infty}\frac{1}{t}\int_0^t T(s)\mathrm{d}s=\frac{\lambda}{k}\quad \text{a.s.}$$

It follows from the comparison theorem of stochastic differential equation [30] that

$$x(t)\leq T(t)\quad \text{a.s.},$$

which yields that

$$\lim_{t\to\infty}\frac{1}{t}\int_0^t x(s)\mathrm{d}s\le\lim_{t\to\infty}\frac{1}{t}\int_0^t T(s)\mathrm{d}s=\frac{\lambda}{k}\quad\text{a.s.}\tag{3.3}$$

By the Itô's formula, we have

$$\mathrm{d}\ln y=\left(p(1-\epsilon)\beta_1 x-\left(k+\epsilon\gamma+\frac{\sigma_2^2}{2}\right)\right)\mathrm{d}t+\sigma_2\mathrm{d}B_2(t).$$

Integrating it from 0 to t and then dividing by t on the both sides, we get

$$\frac{\ln y(t)-\ln y(0)}{t}=\frac{1}{t}\int_0^t\left(p(1-\epsilon)\beta_1 x(s)-\left(k+\epsilon\gamma+\frac{\sigma_2^2}{2}\right)\right)\mathrm{d}s+\frac{1}{t}\int_0^t\sigma_2\mathrm{d}B_2(s).\tag{3.4}$$

Following Eq. (3.3), when $\overline{\mathcal{R}}_{\mathrm{c1}}<1$, we deduce that

$$\begin{aligned}\limsup_{t\to\infty}\frac{\ln y(t)-\ln y(0)}{t}&\le\frac{p(1-\epsilon)\beta_1\lambda}{k}-\left(k+\epsilon\gamma+\frac{\sigma_2^2}{2}\right)\\&=\left(k+\epsilon\gamma+\frac{\sigma_2^2}{2}\right)(\overline{\mathcal{R}}_{\mathrm{c1}}-1)<0,\end{aligned}$$

which means that

$$\limsup_{t\to\infty}\frac{\ln y(t)}{t}<0,\quad\lim_{t\to\infty}y(t)=0\quad\text{a.s.}\tag{3.5}$$

Similarly,

$$\mathrm{d}\ln l=\left(\frac{(1-p)(1-\epsilon)\beta_1 xy}{l}+\beta_2 x+\frac{\epsilon\gamma y}{l}-\left(k+\frac{\sigma_3^2}{2}\right)\right)\mathrm{d}t+\sigma_3\mathrm{d}B_3(t).\tag{3.6}$$

Then, from Eqs. (3.3) and (3.5), we have

$$\limsup_{t\to\infty}\frac{\ln l(t)-\ln l(0)}{t}\le\frac{\beta_2\lambda}{k}-\left(k+\frac{\sigma_3^2}{2}\right)=\left(k+\frac{\sigma_3^2}{2}\right)(\overline{\mathcal{R}}_{\mathrm{c2}}-1),$$

which means that when $\overline{\mathcal{R}}_{\mathrm{c2}}<1$,

$$\limsup_{t\to\infty}\frac{\ln l(t)}{t}<0,\quad\lim_{t\to\infty}l(t)=0\quad\text{a.s.}\tag{3.7}$$

Moreover, from the Eq. (2.2a), we obtain

$$\begin{aligned}\frac{x(t)-x(0)}{t}=\lambda&-\frac{k}{t}\int_0^t x(s)\mathrm{d}s-\frac{(1-\epsilon)\beta_1}{t}\int_0^t x(s)y(s)\mathrm{d}s\\&-\frac{\beta_2}{t}\int_0^t x(s)l(s)\mathrm{d}s+\frac{\sigma_1}{t}\int_0^t x(s)\mathrm{d}B_1(s).\end{aligned}\tag{3.8}$$

Therefore, it follows from Eqs. (3.5), (3.7), (A.1) and (A.2) that

$$\lim_{t\to\infty}\frac{1}{t}\int_0^t x(s)\mathrm{d}s=\frac{\lambda}{k}.$$

Summarizing, if $\overline{\mathcal{R}}_{\mathrm{c}}<1$, then

$$\lim_{t\to\infty}\frac{1}{t}\int_0^t x(s)\mathrm{d}s=\frac{\lambda}{k},\quad \limsup_{t\to\infty}\frac{\ln y(t)}{t}<0,\quad \limsup_{t\to\infty}\frac{\ln l(t)}{t}<0\quad \text{a.s.}$$

The proof is complete. □

Theorem 3.3. *Assume $k>(\sigma_1^2\vee\sigma_2^2\vee\sigma_3^2)/2$. Let $(x(t),y(t),l(t))$ be the solution of model* (2.2) *with the initial condition $(x(0),y(0),l(0))\in\mathbb{R}^3_+$, if $\overline{\mathcal{R}}_{\mathrm{c}}=\overline{\mathcal{R}}_{\mathrm{c2}}>1$, then*

$$\lim_{t\to\infty}\frac{1}{t}\int_0^t x(s)\mathrm{d}s\le\frac{k+\sigma_3^2/2}{\beta_2},\quad \limsup_{t\to\infty}\frac{\ln y(t)}{t}<0,\quad \lim_{t\to\infty}\frac{1}{t}\int_0^t l(s)\mathrm{d}s\ge\frac{k}{\beta_2}\left(\overline{\mathcal{R}}_{\mathrm{c2}}-1\right)>0\quad \textit{a.s.}$$

Namely, the infection will converge to totally latent state with probability one.

Proof. According to Eq. (3.6), we have

$$\mathrm{d}\ln l\ge\left(\beta_2 x-\left(k+\frac{\sigma_3^2}{2}\right)\right)\mathrm{d}t+\sigma_3\mathrm{d}B_3(t),$$

which yields

$$\frac{\ln l(t)-\ln l(0)}{t}\ge\frac{\beta_2}{t}\int_0^t x(s)\mathrm{d}s-\left(k+\frac{\sigma_3^2}{2}\right)+\frac{1}{t}\int_0^t\sigma_3\mathrm{d}B_3(s).$$

Then, we can obtain that

$$\lim_{t\to\infty}\frac{1}{t}\int_0^t x(s)\mathrm{d}s\le\frac{k+\sigma_3^2/2}{\beta_2}.$$

In this way, we conclude from Eq. (3.4) that

$$\frac{\ln y(t)-\ln y(0)}{t}\le\frac{p(1-\epsilon)\beta_1\left(k+\sigma_3^2/2\right)}{\beta_2}-\left(k+\epsilon\gamma+\frac{\sigma_2^2}{2}\right)+\frac{1}{t}\int_0^t\sigma_2\mathrm{d}B_2(s).$$

Hence, when $\overline{\mathcal{R}}_{\mathrm{c1}}<\overline{\mathcal{R}}_{\mathrm{c2}}$,

$$\begin{aligned}\limsup_{t\to\infty}\frac{\ln y(t)}{t}&\le\left(k+\epsilon\gamma+\frac{\sigma_2^2}{2}\right)\left(\frac{p(1-\epsilon)\beta_1\left(k+\sigma_3^2/2\right)}{\beta_2\left(k+\epsilon\gamma+\sigma_2^2/2\right)}-1\right)\\&=\left(k+\epsilon\gamma+\frac{\sigma_2^2}{2}\right)\left(\frac{\overline{\mathcal{R}}_{\mathrm{c1}}}{\overline{\mathcal{R}}_{\mathrm{c2}}}-1\right)<0,\end{aligned}$$

which yields

$$\lim_{t\to\infty} y(t)=0 \quad \text{a.s.}$$

Thus, from Eq. (3.8), we deduce that

$$\frac{x(t)-x(0)}{t}\geq\lambda-\frac{k\left(k+\sigma_3^2/2\right)}{\beta_2}-\frac{\left(k+\sigma_3^2/2\right)}{t}\int_0^t l(s)\mathrm{d}s+\frac{\sigma_1}{t}\int_0^t x(s)\mathrm{d}B_1(s),$$

which reveals that if $\overline{\mathcal{R}}_{c2}>1$ holds,

$$\lim_{t\to\infty}\frac{1}{t}\int_0^t l(s)\mathrm{d}s\geq\frac{1}{k+\sigma_3^2/2}\left(\lambda-\frac{k\left(k+\sigma_3^2/2\right)}{\beta_2}\right)=\frac{k}{\beta_2}(\overline{\mathcal{R}}_{c2}-1)>0.$$

This completes the proof. □

Remark 3.1. Theorem 3.2 gives the sufficient conditions when almost all solutions of model (2.2) tend to the infection-free equilibrium $(\lambda/k,0,0)$, i.e. both productively and latently infected brain macrophages are eliminated. Theorem 3.3 reveals that when $\overline{\mathcal{R}}_c=\overline{\mathcal{R}}_{c2}>1$, latently infected macrophages are present but productively infected brain macrophages are cleared, which demonstrate the existence of HIV-1 brain reservoirs. This is coincide with a phenomenon seen in clinical that the viral loads of HIV-infected patients under efficient cART are undetectable (≤ 50 copies/ml), however, HIV RNA returns to a measurable plasma level when cART is disrupted.

Remark 3.2. It is evident that $\overline{\mathcal{R}}_{c1}\leq\mathcal{R}_{c1}, \overline{\mathcal{R}}_{c2}\leq\mathcal{R}_{c2}$, thus $\overline{\mathcal{R}}_c\leq\mathcal{R}_c$. This indicates that environmental noise leads to a reduction in the basic reproduction number, suggesting that environmental fluctuations can significantly alter the dynamics of HIV-1 infection. We easily find an example when $\overline{\mathcal{R}}_c<1$ but $\mathcal{R}_c>1$ such that the infection exists for ODE model (2.1), all the brain macrophages tend to be healthy for SDE model (2.2). While if $\overline{\mathcal{R}}_c<\mathcal{R}_c<1$, the infection will be eliminated for both model (2.1) and model (2.2). This implies that if all the brain macrophages for ODE model (2.1) tend to be healthy, environmental noises do not affect the viral dynamics in the brain and can be ignored.

3.2 Stochastic persistence via the stationary distribution of model (2.2)

From Hasminskii's ergodic theory [31] and the strong law of large numbers [35], we know that model (2.2) has a unique stationary distribution denoting that the infection is persistent with probability one. In view of this point, next, we will focus on the existence of stationary distribution for model (2.2). And this analysis is usually conducive to motivating our investigation about the influence of environmental noises on the viral dynamics to a large extent.

Theorem 3.4. *If $\overline{\mathcal{R}}_c=\overline{\mathcal{R}}_{c1}>1$ holds, then model (2.2) has a unique stationary distribution.*

Proof. The diffusion matrix associated to model (2.2) is given by

$$\Delta(X)=\big(\alpha_{ij}(X)\big)_{3\times3}=\begin{pmatrix}\sigma_1^2x^2 & 0 & 0\\ 0 & \sigma_2^2y^2 & 0\\ 0 & 0 & \sigma_3^2l^2\end{pmatrix}, \tag{3.9}$$

where $X=(x,y,l)$. Choose

$$E=\min_{(x,y,l)\in\overline{U}\subset\mathbb{R}^3_+}\{\sigma_1^2x^2,\sigma_2^2y^2,\sigma_3^2l^2\},$$

then we have $E>0$, where

$$\overline{U}=\left[\frac{1}{n},n\right]\times\left[\frac{1}{n},n\right]\times\left[\frac{1}{n},n\right].$$

For any $(x,y,l)\in\overline{U}$ and $(\zeta_1,\zeta_2,\zeta_3)\in\mathbb{R}^3_+$, by Eq. (3.9), we have

$$\sum_{i,j=1}^{3}\alpha_{ij}(X)\zeta_i\zeta_j=\sigma_1^2x^2\zeta_1^2+\sigma_2^2y^2\zeta_2^2+\sigma_3^2l^2\zeta_3^2\geq E|\zeta|^2,$$

where $|\zeta|=(\zeta_1^2+\zeta_2^2+\zeta_3^2)^{1/2}$. Then the condition (i) in Lemma A.2 holds.

Define the function

$$W(x,y,l)=M(W_1+W_2)+W_3+W_4,$$

where

$$W_1=-m_1\ln x-\ln y,\qquad W_2=-m_2\ln x-\ln l,$$
$$W_3=m_3(x+y+l)-\ln x-\ln l,\quad W_4=\frac{1}{m_4+1}(x+y+l)^{m_4+1},$$

and $m_i\,(i=1,2,3,4)$ are positive constants which will be determined later. When $\overline{\mathcal{R}}_c=\overline{\mathcal{R}}_{c1}>1$, select suitable constants $M>0$ and $m_4\in(0,1)$ satisfying

$$-M\left(\left(k+\epsilon\gamma+\frac{\sigma_2^2}{2}\right)(\overline{\mathcal{R}}_{c1}-1)+\left(k+\frac{\sigma_3^2}{2}\right)\left(\frac{\overline{\mathcal{R}}_{c1}}{\overline{\mathcal{R}}_{c2}}-1\right)\right)+F_2\leq-2,$$

where

$$F_2=\sup_{(x,y,l)\in\mathbb{R}^3_+}\left\{m_3\lambda+F_0+\big(M(m_1+m_2)+1\big)\left(k+\frac{\sigma_1^2}{2}\right)+\left(k+\frac{\sigma_3^2}{2}\right)\right.$$
$$\left.-\frac{k}{2}x^{m_4+1}-\frac{k}{2}y^{m_4+1}-\frac{k}{2}l^{m_4+1}\right\}<\infty,$$

$$F_0=\sup_{(x,y,l)\in\mathbb{R}^3_+}\left\{\lambda(x+y+l)^{m_4}+\frac{m_4}{2}\left(\sigma_1^2x^{m_4+1}+\sigma_2^2y^{m_4+1}+\sigma_3^2l^{m_4+1}\right)\right.$$
$$\left.-\frac{k}{2}x^{m_4+1}-\frac{k}{2}y^{m_4+1}-\frac{k}{2}l^{m_4+1}\right\}<\infty.$$

It is easy to check that

$$\liminf_{n\to\infty,(x,y,l)\in\mathbb{R}^3_+\setminus U_n}W(x,y,l)=+\infty,$$

where

$$U_n=\left(\frac{1}{n},n\right)\times\left(\frac{1}{n},n\right)\times\left(\frac{1}{n},n\right).$$

Let $(\tilde{x}_0,\tilde{y}_0,\tilde{l}_0)$ be the minimum value point of $W(x,y,l)$. Then we define the nonnegative function

$$\widetilde{W}(x,y,l)=W(x,y,l)-W(\tilde{x}_0,\tilde{y}_0,\tilde{l}_0).$$

By the Itô's formula, we get

$$\begin{aligned}LW_1&=m_1\left(-\frac{\lambda}{x}+(1-\epsilon)\beta_1y+\beta_2l+\left(k+\frac{\sigma_1^2}{2}\right)\right)-p(1-\epsilon)\beta_1x+k+\epsilon\gamma+\frac{\sigma_2^2}{2}\\&\leq-\sqrt{m_1p(1-\epsilon)\beta_1\lambda}+\left(k+\epsilon\gamma+\frac{\sigma_2^2}{2}\right)+m_1\left((1-\epsilon)\beta_1y+\beta_2l+k+\frac{\sigma_1^2}{2}\right).\end{aligned}$$

Choose $m_1=p(1-\epsilon)\beta_1\lambda/k^2$, then

$$\begin{aligned}LW_1&\leq-\frac{p(1-\epsilon)\beta_1\lambda}{k}+\left(k+\epsilon\gamma+\frac{\sigma_2^2}{2}\right)+m_1\left((1-\epsilon)\beta_1y+\beta_2l+k+\frac{\sigma_1^2}{2}\right)\\&=-\left(k+\epsilon\gamma+\frac{\sigma_2^2}{2}\right)(\overline{\mathcal{R}}_{c1}-1)+m_1\left((1-\epsilon)\beta_1y+\beta_2l+k+\frac{\sigma_1^2}{2}\right).\end{aligned}$$

Similarly, we have

$$\begin{aligned}LW_2&=m_2\left(-\frac{\lambda}{x}+(1-\epsilon)\beta_1y+\beta_2l+\left(k+\frac{\sigma_1^2}{2}\right)\right)-\frac{(1-p)(1-\epsilon)\beta_1xy}{l}-\beta_2x-\frac{\epsilon\gamma y}{l}+\left(k+\frac{\sigma_3^2}{2}\right)\\&\leq-\sqrt{m_2\lambda\beta_2}+\left(k+\frac{\sigma_3^2}{2}\right)+m_2(1-\epsilon)\beta_1y+m_2\beta_2l+m_2\left(k+\frac{\sigma_1^2}{2}\right).\end{aligned}$$

Choose

$$m_2=\frac{\beta_1^2p^2(1-\epsilon)^2\left(k+\sigma_3^2/2\right)^4}{\lambda\beta_2^3\left(k+\epsilon\gamma+\sigma_2^2/2\right)^2},$$

then

$$LW_2 \leq -\frac{\beta_1 p(1-\epsilon)\left(k+\sigma_3^2/2\right)^2}{\beta_2\left(k+\epsilon\gamma+\sigma_2^2/2\right)} + \left(k+\frac{\sigma_3^2}{2}\right) + m_2(1-\epsilon)\beta_1 y + m_2\beta_2 l + m_2\left(k+\frac{\sigma_1^2}{2}\right)$$

$$= -\left(k+\frac{\sigma_3^2}{2}\right)\left(\frac{\overline{\mathcal{R}}_{c1}}{\overline{\mathcal{R}}_{c2}}-1\right) + m_2\left((1-\epsilon)\beta_1 y + \beta_2 l + \left(k+\frac{\sigma_1^2}{2}\right)\right).$$

In the same way, we obtain

$$LW_3 = m_3\left(\lambda - k(x+y+l)\right) + (1-\epsilon)\beta_1 y + \beta_2 l + \left(k+\frac{\sigma_1^2}{2}\right) - \frac{\lambda}{x}$$
$$- \frac{(1-p)(1-\epsilon)\beta_1 xy}{l} - \beta_2 x - \frac{\epsilon\gamma y}{l} + \left(k+\frac{\sigma_3^2}{2}\right),$$

$$LW_4 = (x+y+l)^{m_4}\left(\lambda - k(x+y+l)\right) + \frac{m_4}{2}(x+y+l)^{m_4-1}\left(\sigma_1^2 x^2 + \sigma_2^2 y^2 + \sigma_3^2 l^2\right)$$
$$\leq \lambda(x+y+l)^{m_4} - k\left(x^{m_4+1} + y^{m_4+1} + l^{m_4+1}\right) + \frac{m_4}{2}\left(\sigma_1^2 x^{m_4+1} + \sigma_2^2 y^{m_4+1} + \sigma_3^2 l^{m_4+1}\right).$$

Choose

$$m_3 = \frac{\beta_2\left(M(m_1+m_2)+1\right)}{k}, \quad 0 < m_4 < \min\left\{1, \frac{k}{\sigma_1^2} \wedge \frac{k}{\sigma_2^2} \wedge \frac{k}{\sigma_3^2}\right\},$$

then

$$L\widetilde{W} \leq -M\left(k+\epsilon\gamma+\frac{\sigma_2^2}{2}\right)(\overline{\mathcal{R}}_{c1}-1) - M\left(k+\frac{\sigma_3^2}{2}\right)\left(\frac{\overline{\mathcal{R}}_{c1}}{\overline{\mathcal{R}}_{c2}}-1\right) + m_3\lambda - \frac{\lambda}{x} - \frac{\epsilon\gamma y}{l}$$
$$+ \left(M(m_1+m_2)+1\right)(1-\epsilon)\beta_1 y + \left(M(m_1+m_2)+1\right)\left(k+\frac{\sigma_1^2}{2}\right) + \left(k+\frac{\sigma_3^2}{2}\right)$$
$$- \frac{k}{2}x^{m_4+1} - \frac{k}{2}y^{m_4+1} - \frac{k}{2}l^{m_4+1} + F_0.$$

Next, we construct a compact subset D such that the condition (ii) in Lemma A.2 holds. Define the bounded closed set

$$D := \left\{(x,y,l) : \varepsilon_1 \leq x \leq \frac{1}{\varepsilon_1}, \varepsilon_2 \leq y \leq \frac{1}{\varepsilon_2}, \varepsilon_3 \leq l \leq \frac{1}{\varepsilon_3}\right\},$$

where ε_i $(i=1,2,3)$ are sufficiently small constants. We choose ε_i $(i=1,2,3)$ satisfying the following conditions:

$$-\frac{\lambda}{\varepsilon_1} + F_1 \leq -1,$$

$$
\begin{aligned}
&-M\left(\left(k+\epsilon\gamma+\frac{\sigma_2^2}{2}\right)(\overline{\mathcal{R}}_{c1}-1)+\left(k+\frac{\sigma_3^2}{2}\right)\left(\frac{\overline{\mathcal{R}}_{c1}}{\overline{\mathcal{R}}_{c2}}-1\right)\right)\\
&\quad+\big(M(m_1+m_2)+1\big)(1-\epsilon)\beta_1\varepsilon_2+F_2\le-1,\\
&-\frac{\epsilon\gamma\varepsilon_2}{\varepsilon_3}+F_1\le-1,\quad -\frac{k}{4\varepsilon_1^{m_4+1}}+F_1\le-1,\quad -\frac{k}{4\varepsilon_2^{m_4+1}}+F_1\le-1,\quad -\frac{k}{4\varepsilon_3^{m_4+1}}+F_1\le-1,
\end{aligned}
$$

where

$$
\begin{aligned}
F_1=\sup_{(x,y,l)\in\mathbb{R}^3_+}\Bigg\{&\big(M(m_1+m_2)+1\big)(1-\epsilon)\beta_1 y+m_3\lambda+F_0+\big(M(m_1+m_2)+1\big)\left(k+\frac{\sigma_1^2}{2}\right)\\
&+\left(k+\frac{\sigma_3^2}{2}\right)-\frac{k}{4}x^{m_4+1}-\frac{k}{4}y^{m_4+1}-\frac{k}{4}l^{m_4+1}\Bigg\}<\infty.
\end{aligned}
$$

For convenience, we divide $\mathbb{R}^3_+\setminus D$ into six domains

$$
\begin{aligned}
&D_1=\big\{(x,y,l)\in\mathbb{R}^3_+,0<x<\varepsilon_1\big\}, && D_2=\big\{(x,y,l)\in\mathbb{R}^3_+,0<y<\varepsilon_2,x\ge\varepsilon_1\big\},\\
&D_3=\big\{(x,y,l)\in\mathbb{R}^3_+,0<l<\varepsilon_3,x\ge\varepsilon_1,y\ge\varepsilon_2\big\}, && D_4=\left\{(x,y,l)\in\mathbb{R}^3_+,x\ge\frac{1}{\varepsilon_1}\right\},\\
&D_5=\left\{(x,y,l)\in\mathbb{R}^3_+,y\ge\frac{1}{\varepsilon_2}\right\}, && D_6=\left\{(x,y,l)\in\mathbb{R}^3_+,l\ge\frac{1}{\varepsilon_3}\right\}.
\end{aligned}
$$

We will prove that $L\widetilde{W}(x,y,l)\le-1$ on $\mathbb{R}^3_+\setminus D$, which is equivalent to show it on the above six domains.

Case 1: If $(x,y,l)\in D_1$, we can obtain

$$
L\widetilde{W}\le-\frac{\lambda}{x}+F_1\le-\frac{\lambda}{\varepsilon_1}+F_1\le-1.
$$

Case 2: If $(x,y,l)\in D_2$, we can obtain

$$
\begin{aligned}
L\widetilde{W}&\le-M\left(\left(k+\epsilon\gamma+\frac{\sigma_2^2}{2}\right)(\overline{\mathcal{R}}_{c1}-1)+\left(k+\frac{\sigma_3^2}{2}\right)\left(\frac{\overline{\mathcal{R}}_{c1}}{\overline{\mathcal{R}}_{c2}}-1\right)\right)\\
&\quad+\big(M(m_1+m_2)+1\big)(1-\epsilon)\beta_1 y+F_2\\
&\le-M\left(\left(k+\epsilon\gamma+\frac{\sigma_2^2}{2}\right)(\overline{\mathcal{R}}_{c1}-1)+\left(k+\frac{\sigma_3^2}{2}\right)\left(\frac{\overline{\mathcal{R}}_{c1}}{\overline{\mathcal{R}}_{c2}}-1\right)\right)\\
&\quad+\big(M(m_1+m_2)+1\big)(1-\epsilon)\beta_1\varepsilon_2+F_2\le-1.
\end{aligned}
$$

Case 3: If $(x,y,l)\in D_3$, we can obtain

$$
L\widetilde{W}\le-\frac{\epsilon\gamma y}{l}+F_1\le-\frac{\epsilon\gamma\varepsilon_2}{\varepsilon_3}+F_1\le-1.
$$

Case 4: If $(x,y,l)\in D_4$, we can obtain

$$L\widetilde{W}\leq -\frac{k}{4}x^{m_4+1}+F_1\leq -\frac{k}{4\varepsilon_1^{m_4+1}}+F_1\leq -1.$$

Case 5: If $(x,y,l)\in D_5$, we can obtain

$$L\widetilde{W}\leq -\frac{k}{4}y^{m_4+1}+F_1\leq -\frac{k}{4\varepsilon_2^{m_4+1}}+F_1\leq -1.$$

Case 6: If $(x,y,l)\in D_6$, we can obtain

$$L\widetilde{W}\leq -\frac{k}{4}l^{m_4+1}+F_1\leq -\frac{k}{4\varepsilon_3^{m_4+1}}+F_1\leq -1.$$

Hence,

$$L\widetilde{W}\leq -1,\quad \forall (x,y,l)\in \mathbb{R}^3_+\setminus D.$$

Therefore, according to Lemma A.2, one can get that model (2.2) has a unique stationary distribution. This completes the proof. □

Remark 3.3. Theorem 3.4 declares the fact that when $\overline{\mathcal{R}}_c=\overline{\mathcal{R}}_{c1}>1$, model (2.2) has a unique stationary distribution, which means that both productively and latently infected brain macrophages are present, i.e. the HIV-1 will persist with probability one. Considering Remark 3.1 again, we can conclude that, Theorems 3.2-3.4 give the threshold dynamics of model (2.2).

3.3 Probability density function

From Theorem 3.4, we can see that, when $\overline{\mathcal{R}}_c=\overline{\mathcal{R}}_{c1}>1$, model (2.2) admits a stationary distribution. In this subsection, we are committed to looking for the probability density function to further study the dynamic characteristics of the model from the perspective of statistics.

Let $s_1=\ln x, s_2=\ln y, s_3=\ln l$. By Itô's formula, we obtain the equivalent model of model (2.2)

$$\begin{cases} \mathrm{d}s_1=\left(\lambda e^{-s_1}-(1-\epsilon)\beta_1 e^{s_2}-\beta_2 e^{s_3}-\left(k+\dfrac{\sigma_1^2}{2}\right)\right)\mathrm{d}t+\sigma_1\mathrm{d}B_1(t),\\ \mathrm{d}s_2=\left(p(1-\epsilon)\beta_1 e^{s_1}-\left(k+\varepsilon\gamma+\dfrac{\sigma_2^2}{2}\right)\right)\mathrm{d}t+\sigma_2\mathrm{d}B_2(t),\\ \mathrm{d}s_3=\left((1-p)(1-\epsilon)\beta_1 e^{s_1+s_2-s_3}+\beta_2 e^{s_1}+\epsilon\gamma e^{s_2-s_3}-\left(k+\dfrac{\sigma_3^2}{2}\right)\right)\mathrm{d}t+\sigma_3\mathrm{d}B_3(t). \end{cases} \tag{3.10}$$

If

$$\widehat{\mathcal{R}}_{c1}=\frac{p(1-\epsilon)\beta_1\lambda}{\left(k+\sigma_1^2/2\right)\left(k+\epsilon\gamma+\sigma_2^2/2\right)}>1$$

and $\overline{\mathcal{R}}_{c1}>\overline{\mathcal{R}}_{c2}$ hold, model (2.2) admits a quasi-steady state $\overline{P}_1=(\overline{x}_1,\overline{y}_1,\overline{l}_1)=(e^{s_1^*},e^{s_2^*},e^{s_3^*})$, where

$$\begin{aligned}
&\overline{x}_1=\frac{\epsilon\gamma+k+\sigma_2^2/2}{p\beta_1(1-\epsilon)},\\
&\overline{y}_1=\frac{\left(p(1-\epsilon)\beta_1\lambda-\left(k+\sigma_1^2/2\right)\left(k+\epsilon\gamma+\sigma_2^2/2\right)\right)\left(\beta_1 p(1-\epsilon)\left(k+\sigma_3^2/2\right)-\beta_2\left(k+\epsilon\gamma+\sigma_2^2/2\right)\right)}{p\beta_1(1-\epsilon)\Big(\beta_1(1-\epsilon)\left(k+\sigma_3^2/2\right)-\beta_2\left(k+\sigma_2^2/2\right)\Big)\left(k+\epsilon\gamma+\sigma_2^2/2\right)},\\
&\overline{l}_1=\frac{\left((1-p)\left(k+\sigma_2^2/2\right)+\epsilon\gamma\right)\left(p(1-\epsilon)\beta_1\lambda-\left(k+\sigma_1^2/2\right)\left(k+\epsilon\gamma+\sigma_2^2/2\right)\right)}{p\left(k+\epsilon\gamma+\sigma_2^2/2\right)\left(\beta_1(1-\epsilon)\left(k+\sigma_3^2/2\right)-\beta_2\left(k+\sigma_2^2/2\right)\right)}.
\end{aligned}$$

It is obvious that $\overline{P}_1$ is consistent with positive equilibrium P_1 of ODE model (2.1) when $\sigma_i=0$ $(i=1,2,3)$.

Let

$$v_i=s_i-s_i^*,\quad i=1,2,3, \tag{3.11}$$

where $s_1^*=\ln\overline{x}_1, s_2^*=\ln\overline{y}_1, s_3^*=\ln\overline{l}_1$. Then the linearized system of model (3.10) is as follows:

$$\begin{cases}
\mathrm{d}v_1=(-a_{11}v_1-a_{12}v_2-a_{13}v_3)\mathrm{d}t+\sigma_1\mathrm{d}B_1(t),\\
\mathrm{d}v_2=a_{21}v_1\mathrm{d}t+\sigma_2\mathrm{d}B_2(t),\\
\mathrm{d}v_3=(a_{31}v_1+a_{32}v_2-a_{32}v_3)\mathrm{d}t+\sigma_3\mathrm{d}B_3(t),
\end{cases} \tag{3.12}$$

where

$$\begin{aligned}
&a_{11}=\lambda e^{-s_1^*}>0,\quad a_{12}=(1-\epsilon)\beta_1 e^{s_2^*}>0,\\
&a_{13}=\beta_2 e^{s_3^*}>0,\quad a_{21}=p(1-\epsilon)\beta_1 e^{s_1^*}>0,\\
&a_{31}=(1-p)(1-\epsilon)\beta_1 e^{s_1^*+s_2^*-s_3^*}+\beta_2 e^{s_1^*}>0,\\
&a_{32}=(1-p)(1-\epsilon)\beta_1 e^{s_1^*+s_2^*-s_3^*}+\epsilon\gamma e^{s_2^*-s_3^*}>0.
\end{aligned}$$

Next, applying Lemmas A.3 and A.4, we show the local probability density function of model (2.2) near the quasi-steady equilibrium $\overline{P}_1$ which is presented in Theorem 3.5.

Theorem 3.5. *Let $(v_1(t),v_2(t),v_3(t))$ be a solution of model* (3.12) *with any initial value $(v_1(0),$ $v_2(0),$ $v_3(0))\in\mathbb{R}^3$. If $\widehat{\mathcal{R}}_{c1}>1$ and $\overline{\mathcal{R}}_{c1}>\overline{\mathcal{R}}_{c2}$ hold, there is a probability density function $\Phi(v_1,v_2,v_3)$ around the quasi-steady state $\overline{P}_1$, which can be expressed in the following form:*

$$\Phi(v_1,v_2,v_3)=(2\pi)^{-\frac{3}{2}}|\Sigma|^{-\frac{1}{2}}e^{-\frac{1}{2}(v_1,v_2,v_3)\Sigma^{-1}(v_1,v_2,v_3)^\top},$$

in which Σ is positive definite, and

(1) if $w_1\neq 0$ and $w_2\neq 0$, then

$$\Sigma=\rho_{11}^2(M_{11}I_1J_1)^{-1}\Sigma_0\big((M_{11}I_1J_1)^{-1}\big)^\top+\rho_{21}^2(M_{21}I_2J_2)^{-1}\Sigma_0\big((M_{21}I_2J_2)^{-1}\big)^\top +\rho_3^2(M_3J_3)^{-1}\Sigma_0\big((M_3J_3)^{-1}\big)^\top;$$

(2) if $w_1\neq 0$ and $w_2=0$, then

$$\Sigma=\rho_{11}^2(M_{11}I_1J_1)^{-1}\Sigma_0\big((M_{11}I_1J_1)^{-1}\big)^\top+\rho_{22}^2(M_{22}I_2J_2)^{-1}\bar{\Theta}_0\big((M_{22}I_2J_2)^{-1}\big)^\top +\rho_3^2(M_3J_3)^{-1}\Sigma_0\big((M_3J_3)^{-1}\big)^\top;$$

(3) if $w_1=0$ and $w_2\neq 0$, then

$$\Sigma=\rho_{12}^2(M_{12}I_1J_1)^{-1}\Theta_0\big((M_{12}I_1J_1)^{-1}\big)^\top+\rho_{21}^2(M_{21}I_2J_2)^{-1}\Sigma_0\big((M_{21}I_2J_2)^{-1}\big)^\top +\rho_3^2(M_3J_3)^{-1}\Sigma_0\big((M_3J_3)^{-1}\big)^\top;$$

(4) if $w_1=0$ and $w_2=0$, then

$$\Sigma=\rho_{12}^2(M_{12}I_1J_1)^{-1}\Theta_0\big((M_{12}I_1J_1)^{-1}\big)^\top+\rho_{22}^2(M_{22}I_2J_2)^{-1}\bar{\Theta}_0\big((M_{22}I_2J_2)^{-1}\big)^\top +\rho_3^2(M_3J_3)^{-1}\Sigma_0\big((M_3J_3)^{-1}\big)^\top.$$

Here,

$$w_1=-\frac{a_{21}a_{32}(a_{21}-a_{31})}{a_{31}^2},\quad w_2=\frac{a_{11}a_{12}a_{32}-a_{12}^2a_{31}-a_{12}a_{32}^2-a_{13}a_{32}^2}{a_{32}^2},$$

and other parameters are provided in the proof of this theorem.

For simplicity, we put the proof of Theorem 3.5 in Appendix B.

Theorem 3.6. *Let $(x(t),y(t),l(t))$ be a solution of model (2.2) with any initial value $(x(0),y(0),l(0))\in\mathbb{R}^3$. Another way to state Theorem 3.5 is that if $\widehat{\mathcal{R}}_{c1}>1$ and $\overline{\mathcal{R}}_{c1}>\overline{\mathcal{R}}_{c2}$ hold, there is a probability density function $\Phi(x,y,l)$ around the quasi-steady state $\overline{P}_1$, which can be expressed in the following form:*

$$\Phi(x,y,l)=(2\pi)^{-\frac{3}{2}}|\Sigma|^{-\frac{1}{2}}(xyl)^{-1}e^{-\frac{1}{2}(\ln\frac{x}{\bar{x}_1},\ln\frac{y}{\bar{y}_1},\ln\frac{l}{\bar{l}_1})\Sigma^{-1}(\ln\frac{x}{\bar{x}_1},\ln\frac{y}{\bar{y}_1},\ln\frac{l}{\bar{l}_1})^\top},$$

and Σ is defined in Theorem 3.5.

Remark 3.4. It is worth pointing out that the marginal density functions of $\Phi(x,y,l)$ with respect to x,y and l are as follows:

$$\begin{aligned}\Upsilon(x)&=\frac{1}{x\sqrt{2\pi\varpi_{11}}}\exp\left(-\frac{(\ln x-\ln\bar{x}_1)^2}{2\varpi_{11}}\right),\\ \Upsilon(y)&=\frac{1}{y\sqrt{2\pi\varpi_{22}}}\exp\left(-\frac{(\ln y-\ln\bar{y}_1)^2}{2\varpi_{22}}\right),\\ \Upsilon(l)&=\frac{1}{l\sqrt{2\pi\varpi_{33}}}\exp\left(-\frac{(\ln l-\ln\bar{l}_1)^2}{2\varpi_{33}}\right),\end{aligned}\tag{3.13}$$

where ϖ_{11},ϖ_{22} and ϖ_{33} are defined in the proof of Theorem 3.5 in Appendix B.

4 Numerical simulations

In this section, we perform some numerical simulations to discuss how environmental noises affect the dynamics of latently and productively infected brain macrophages during viral infection. Here, we apply the Milstein method to solve the SDE model (2.2). The timestep is set as $h=0.002$, which is sufficiently small to accurately approximate the stochastic dynamics and improve numerical stability. Following [41], the parameter values of SDE model (2.2) are given in Table 2. According to Theorems 3.2 and 3.3, our discussion will be conducted under the premise of $k>(\sigma_1^2\vee\sigma_2^2\vee\sigma_3^2)/2$, i.e. $\sigma_1\vee\sigma_2\vee\sigma_3\in(0,2.98)$. We note that the variations in the deactivated rate γ may lead to dynamic differences, so we conduct numerical experiments by adopting different parameter values within the corresponding range $(27.8,152)$, as proposed in [41].

Table 2: The values of the parameters of the SDE model (2.2).

Paras	Range	Value	Unit	Source
λ	$[1.32\times10^6,3.7\times10^7]$	9.4785×10^6	per g	[40,41]
β_1	$[5.75\times10^{-6},1.52\times10^{-5}]$	1.17×10^{-5}	per year	[40,41]
β_2	$[2.92\times10^{-7},4.18\times10^{-6}]$	2.23×10^{-6}	per year	[41]
k	$[0.627,9.84]$	4.45	per year	[40,41]
ϵ	$[0.150,0.654]$	0.152	unit-free	[41]
p	$[0,1]$	0.5	unit-free	[41]
x_0	$[2.09\times10^6,3.85\times10^6]$	2.13×10^6	per g	[3,41]
y_0	$[9.06,11.1]$	11.0	per g	[24,41]
l_0	$[0,1.0\times10^6]$	0	per g	[41]

Example 4.1. When we adopt $\gamma=35$, then simple calculation shows that

$$\mathcal{R}_{c1}=1.0815,\quad \mathcal{R}_{c2}=1.0674,\quad \mathcal{R}_c=1.0815,$$

which means that ODE model (2.1) has a infection-free equilibrium $P_0=(2.130\times10^6,0,0)$, a latent equilibrium $P_2=(1.996\times10^6,0,1.345\times10^5)$, and a globally asymptotically stable productive equilibrium $P_1=(1.969\times10^6,616.326,1.599\times10^5)$.

If $(\sigma_1,\sigma_2,\sigma_3)=(0.05,0.05,0.10)$, then $\overline{\mathcal{R}}_c>\widehat{\mathcal{R}}_{c1}=1.0811>1$ and $\overline{\mathcal{R}}_{c1}>\overline{\mathcal{R}}_{c2}$ (the second column in Table 3). From Theorem 3.4, we know that model (2.2) admits a unique stationary distribution, i.e. the HIV-1 infection is persistent with probability one. Figs. 1(a) and 1(b) show the simple paths of ODE model (2.1) together with the numerical results of 100 stochastic simulations and the corresponding average values, which suggest that the solution of SDE model (2.2) fluctuates around the productive equilibrium P_1. That is to say, in this case, both productively and latently infected macrophages are present with probability one. According to Theorem 3.6 and Remark 3.4, the distribution admits a probability density function around the quasi-steady state $\overline{P}_1=(1.97\times10^6,6.59\times10^2,1.59\times10^5)$, and the marginal density functions are given by

$$\Upsilon(x)=\frac{21.87}{x}\exp\left(-1502.60\left(\ln\left(\frac{x}{1.97\times10^{6}}\right)\right)^{2}\right),$$
$$\Upsilon(y)=\frac{0.96}{y}\exp\left(-2.92\left(\ln\left(\frac{y}{6.59\times10^{2}}\right)\right)^{2}\right),$$
$$\Upsilon(l)=\frac{3.01}{l}\exp\left(-28.41\left(\ln\left(\frac{l}{1.59\times10^{5}}\right)\right)^{2}\right),$$

Table 3: The values of $\overline{\mathcal{R}}_{c1}$, $\overline{\mathcal{R}}_{c2}$ and $\overline{\mathcal{R}}_{c}$ when $\gamma=35$.

$(\sigma_1,\sigma_2,\sigma_3)$	(0.05, 0.05, 0.10)	(0.05, 1.20, 0.70)	(0.05,2.00,1.50)
$\overline{\mathcal{R}}_{c1}$	1.0814	1.0073	0.8975
$\overline{\mathcal{R}}_{c2}$	1.0662	1.0117	0.8520
$\overline{\mathcal{R}}_{c}$	1.0814	1.0117	0.8975

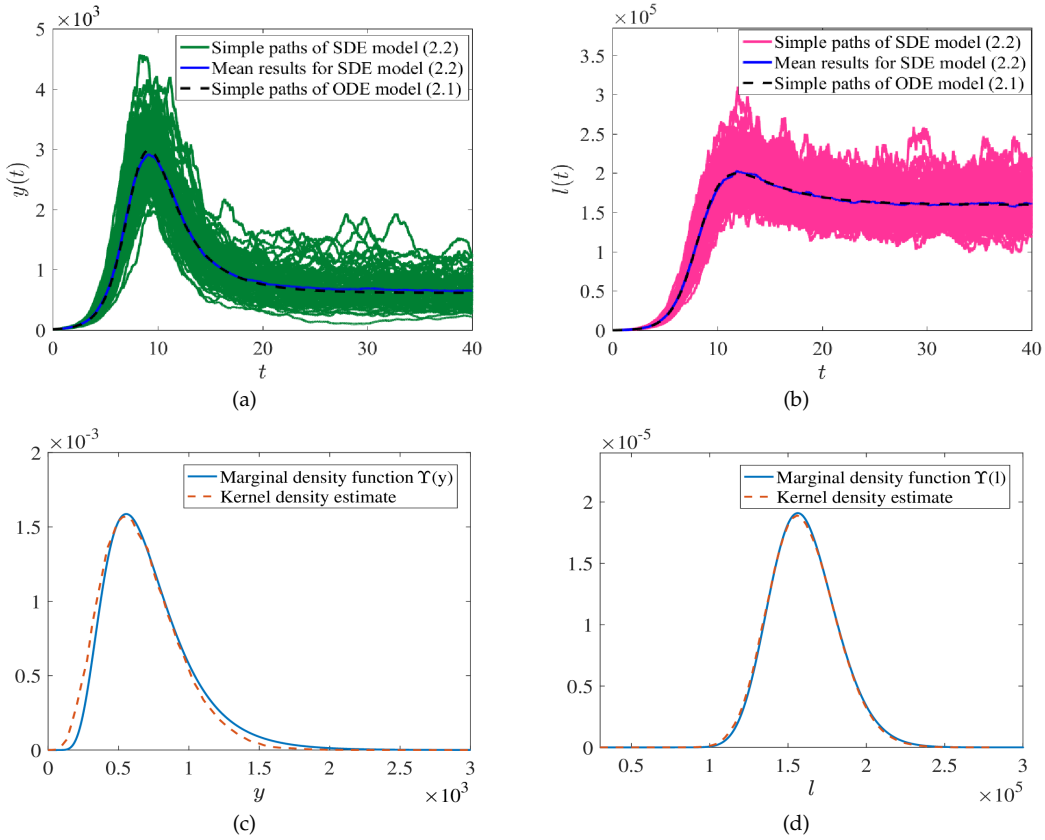

Figure 1: The dynamics of $y(t)$ and $l(t)$ for SDE model (2.2) with $\gamma=35$ when $(\sigma_1,\sigma_2,\sigma_3)=(0.05,0.05,0.10)$. (a), (b) Time-series plots; (c), (d) Kernel density estimates and marginal density functions.

which is shown numerically by the blue solid lines in Figs. 1(c) and 1(d). For comparison, we present the kernel density estimates (orange dashed lines) obtained from 4,000,000 simulations of model (2.2) at $t=4{,}000$, using Matlab's `ksdensity` function. The close agreement between the theoretical and simulated results validates the correctness of the theoretical analysis.

Next, we increase the value of noise intensities $(\sigma_1,\sigma_2,\sigma_3)$ to $(0.05,1.20,0.70)$ and $(0.05,2.00,1.50)$, respectively, and the corresponding values of $\overline{\mathcal{R}}_{c1}$, $\overline{\mathcal{R}}_{c2}$ and $\overline{\mathcal{R}}_c$ are shown in the third and fourth columns of Table 3. One can see that, in the case of small noise intensities, i.e. $(\sigma_1,\sigma_2,\sigma_3)=(0.05,1.20,0.70)$, all the profiles show that the productively infected brain macrophages will be cleared with probability one, which is supported by the numerical simulations displayed in Figs. 2(a) and 2(b). In the case of the larger noise intensities $(\sigma_1,\sigma_2,\sigma_3)=(0.05,2.00,1.50)$ that makes $\overline{\mathcal{R}}_c<1$, the profiles in Figs. 2(c) and 2(d) demonstrate that both productively and latently infected macrophages will be eliminated almost surely.

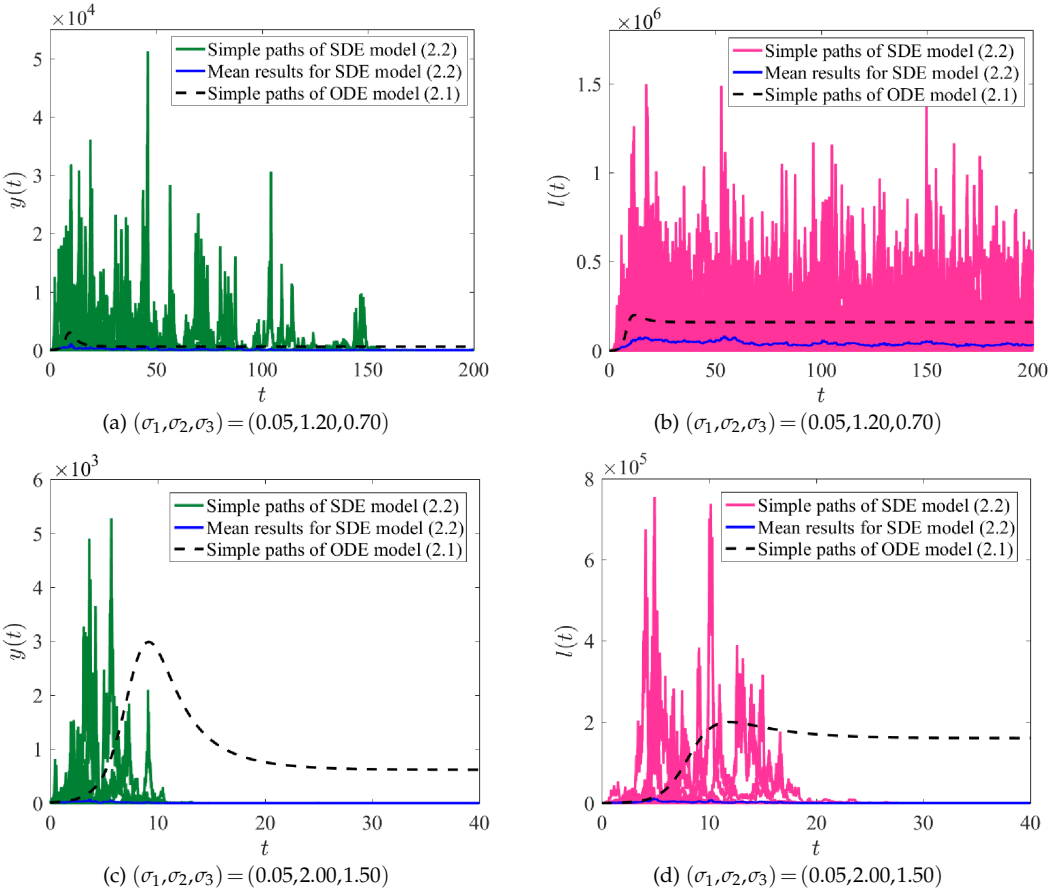

(a) $(\sigma_1,\sigma_2,\sigma_3)=(0.05,1.20,0.70)$ (b) $(\sigma_1,\sigma_2,\sigma_3)=(0.05,1.20,0.70)$

(c) $(\sigma_1,\sigma_2,\sigma_3)=(0.05,2.00,1.50)$ (d) $(\sigma_1,\sigma_2,\sigma_3)=(0.05,2.00,1.50)$

Figure 2: The dynamics of $y(t)$ and $l(t)$ for SDE model (2.2) with $\gamma=35$.

In a simple summary, the numerical results above show that, as expected, environment noise is beneficial for suppressing the outbreak of the virus infection in the brain. However, this is not always true.

Example 4.2. When we adopt $\gamma=38$, then simple calculation shows that

$$\mathcal{R}_{c1}=1.0333, \quad \mathcal{R}_{c2}=1.0674, \quad \mathcal{R}_{c}=1.0674,$$

which means that ODE model (2.1) has a infection-free equilibrium $P_0=(2.130\times10^6,0,0)$ and a globally asymptotically stable latent equilibrium $P_2=(1.996\times10^6,0,1.345\times10^5)$, which means that the productively infected brain macrophages will be eliminated.

When $(\sigma_1,\sigma_2,\sigma_3)=(0.05,0.05,0.60)$, we have $\overline{\mathcal{R}}_c=1.0332>1$ and $\overline{\mathcal{R}}_{c1}>\overline{\mathcal{R}}_{c2}=1.0259$. According to Theorem 3.4, both productively and latently infected macrophages are present with probability one (Fig. 3). This reveals that the white noises may bring about an outbreak of virus infection. Simply speaking, environmental noise is not conducive to controlling HIV-1 infection in the brain.

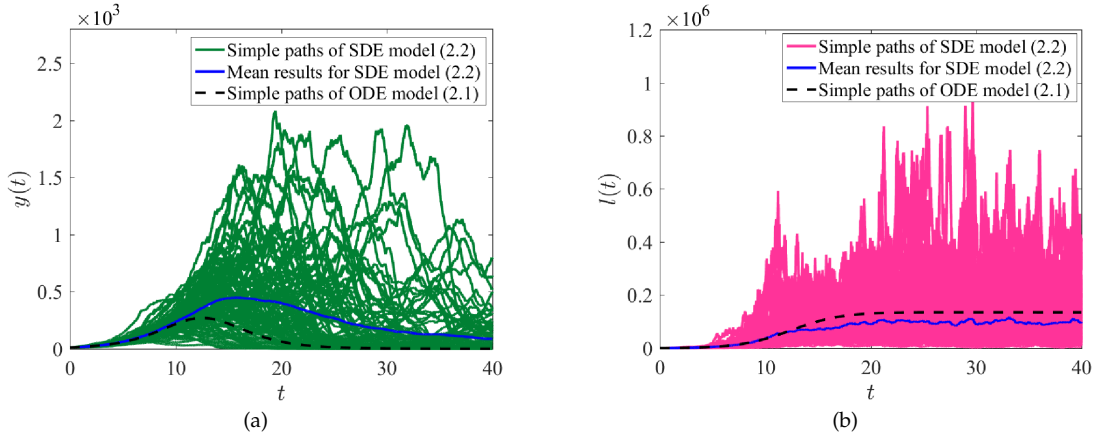

Figure 3: The dynamics of $y(t)$ and $I(t)$ for SDE model (2.2) with $\gamma=38$ and $(\sigma_1,\sigma_2,\sigma_3)=(0.05,0.05,0.60)$.

5 Concluding remarks

This study develops a stochastic HIV-1 infection model (2.2) to delineate viral dynamics in brain macrophages under environmental noise. By design, the model isolates intrinsic noise effects during cART-suppressed infection – a feature difficult to quantify clinically due to confounders like host heterogeneity and drug penetration gradients. Through systematic comparison with the deterministic counterpart (2.1) and analysis of the inequalities $\overline{\mathcal{R}}_{c1}\leq\mathcal{R}_{c1}, \overline{\mathcal{R}}_{c2}\leq\mathcal{R}_{c2}$, we demonstrate how noise reshapes system behavior. Fig. 4 reveals three dynamical regimes demarcated by the ODE solution (blue lines), with stochastic trajectories exhibiting:

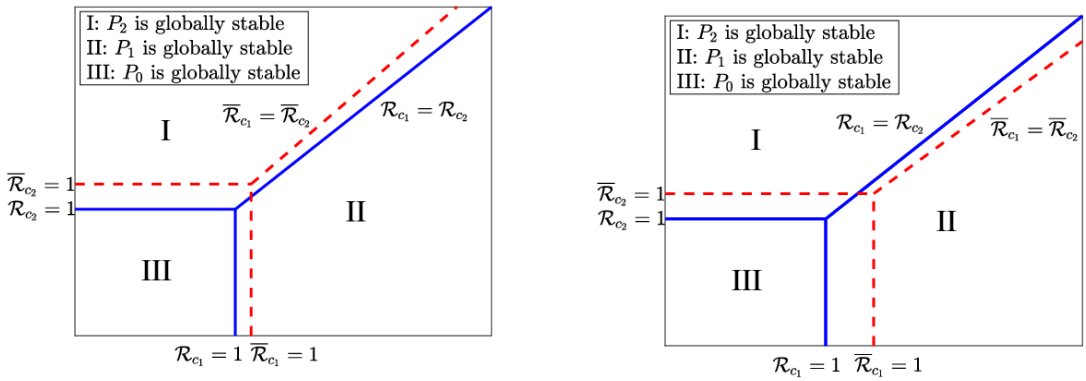

Figure 4: The relations between the parameter regions of distinct model outcomes based on the dynamic behavior of ODE model (2.1) and SDE model (2.2). The blue (dynamic transition line of model (2.1))/ red (dynamic transition line of model (2.2)) lines divide the diagram into three regions.

(1) **Region I** ($\mathcal{R}_c = \mathcal{R}_{c2} > 1$):

- $\mathcal{R}_c > \overline{\mathcal{R}}_c = \overline{\mathcal{R}}_{c2} > 1$: Latent infection dominance (Theorem 3.3)
- $\mathcal{R}_c > \overline{\mathcal{R}}_c = \overline{\mathcal{R}}_{c1} > 1$: Coexistence of productive and latent infection (Theorem 3.4 and Figs. 3, 4(a))
- $\mathcal{R}_c > 1 > \overline{\mathcal{R}}_c$: Viral clearance (Theorem 3.2)

(2) **Region II** ($\mathcal{R}_c = \mathcal{R}_{c1} > 1$):

- $\mathcal{R}_c > \overline{\mathcal{R}}_c = \overline{\mathcal{R}}_{c1} > 1$: Coexistence state (Theorem 3.4 and Figs. 1(a)-(b))
- $\mathcal{R}_c > \overline{\mathcal{R}}_c = \overline{\mathcal{R}}_{c2} > 1$: Latency stabilization (Theorem 3.3 and Figs. 2(a)-(b), 4(b))
- $\mathcal{R}_c > 1 > \overline{\mathcal{R}}_c$: Infection-free state (Theorem 3.2 and Figs. 2(c)-(d))

(3) **Region III** ($\mathcal{R}_c < 1$): Global viral extinction in both models (Theorem 3.2).

It is worthy to point out that our study establishes a unified mechanistic framework linking stochastic viral dynamics to clinical observations in HIV neuropathogenesis. The derived thresholds $\overline{\mathcal{R}}_{c1}$ and $\overline{\mathcal{R}}_{c2}$ provide critical, experimentally testable predictions: while $\overline{\mathcal{R}}_c = \overline{\mathcal{R}}_{c2} > 1$ explains persistent neuroinflammation despite undetectable plasma viremia through stochastic latency dynamics [23], $\overline{\mathcal{R}}_c = \overline{\mathcal{R}}_{c1} > 1$ accounts for CSF viral rebound post-cART and viral blips during suppressive therapy [15]. This noise-induced duality – where stochastic fluctuations can either promote viral clearance or sustain reservoir persistence – resolves the apparent paradox of compartmentalized HIV progression in the CNS. Importantly, our model bridges experimental and clinical findings, demonstrating consistency with neuropathological evidence of latency [1] and primate studies of latent SIV reservoirs [4], thereby offering a unified explanation for both HAND progression and the observed heterogeneity in treatment outcomes.

Furthermore, to bridge modeling with translational research, future work will:

(1) Integrate single-cell transcriptomics of brain macrophages to parameterize infectivity heterogeneity.

(2) Characterize viral bottlenecks using CSF quasispecies data.

(3) Calibrate the model using clinical cohorts on viral rebound kinetics post-cART (e.g. AIDS Clinical Trials Group, ACTG). Such empirical synergy could refine our understanding of noise-driven HIV-1 dynamics in CNS reservoirs.

Appendix A. Preliminaries

Here, we first give the following lemma. The proof is standard, so we refer the reader to [57] for verification.

Lemma A.1. *Assume* $k>(\sigma_1^2\vee\sigma_2^2\vee\sigma_3^2)/2$. *Let* $(x(t),y(t),l(t))$ *be the solution of model* (2.2) *with the initial value* $(x(0),y(0),l(0))\in\mathbb{R}^3_+$. *Then*

$$\lim_{t\to\infty}\frac{x(t)}{t}=0,\qquad \lim_{t\to\infty}\frac{y(t)}{t}=0,\qquad \lim_{t\to\infty}\frac{l(t)}{t}=0\qquad a.s., \tag{A.1}$$

$$\lim_{t\to\infty}\frac{\int_0^t x(s)\mathrm{d}B_1(s)}{t}=0,\quad \lim_{t\to\infty}\frac{\int_0^t y(s)\mathrm{d}B_2(s)}{t}=0,\quad \lim_{t\to\infty}\frac{\int_0^t l(s)\mathrm{d}B_3(s)}{t}=0\quad a.s. \tag{A.2}$$

Based on the work proposed by Khasminskii, the following lemma summarizes the results concerning the existence of the stationary distribution, which can be found in [31].

Let $X(t)$ be a regular time-homogeneous Markov process in $\mathbb{R}^l$ described by the following stochastic differential equation:

$$\mathrm{d}X(t)=b(X)\mathrm{d}t+\sum_{r=1}^{k}g_r(X)\mathrm{d}B_r(t). \tag{A.3}$$

The diffusion matrix is defined as follows:

$$B(X)=\big(\big(b_{ij}(X)\big)\big),\quad b_{ij}(X)=\sum_{r=1}^{k}g_r^i(X)g_r^j(X), \tag{A.4}$$

where $X(t)$ is nonsingular.

Lemma A.2. *If there exists a bounded open domain* $U\subset\mathbb{R}^l$ *with regular boundary* Γ, *having the following properties:*

(i) In the domain U *and some neighborhood thereof, the smallest eigenvalue of the diffusion matrix* $B(X)$ *is bounded away from zero.*

(ii) If $X\in\mathbb{R}^l\setminus U$, *the mean time* τ *at which a path issuing from* X *reaches the set* U *is finite, and* $\sup_{X\in K}\mathbb{E}^X\tau<\infty$ *for every compact subset* $K\subset\mathbb{R}^l$, *then the Markov process* $X(t)$ *has a stationary distribution.*

Finally, in order to get the expression of probability density function, we require the following lemmas which are announced without proofs in [58].

Lemma A.3. *Consider the algebraic equation* $G_0^2+A_0\Sigma_0+\Sigma_0A_0^\top=0$, *where* $G_0=\mathrm{diag}(1,0,0)$,

$$A_0=\begin{pmatrix}-a_1 & -a_2 & -a_3\\ 1 & 0 & 0\\ 0 & 1 & 0\end{pmatrix}.$$

If $a_1>0,a_3>0$ *and* $a_1a_2-a_3>0$, *then the matrix* Σ_0 *is positive definite. In this case, the matrix of the form* A_0 *is called the standard* R_1 *matrix.*

Lemma A.4. *Consider the algebraic equation* $G_0^2+B_0\Theta_0+\Theta_0B_0^\top=0$, *where* $G_0=\mathrm{diag}(1,0,0)$,

$$B_0=\begin{pmatrix}-b_1 & -b_2 & -b_3\\ 1 & 0 & 0\\ 0 & 0 & b_{33}\end{pmatrix}.$$

If $b_1>0$ *and* $b_2>0$, *then the matrix* Θ_0 *is positive semi-definite. In this case, the matrix of the form* B_0 *is called the standard* R_2 *matrix.*

Appendix B. The proof of Theorem 3.5

Proof. In view of model (3.12), we rewrite model (3.12) in the following form:

$$\mathrm{d}V=AV\mathrm{d}t+G\mathrm{d}B(t),$$

where

$$V=(v_1,v_2,v_3)^\top,\quad G=\mathrm{diag}(\sigma_1,\sigma_2,\sigma_3),\quad B(t)=\big(B_1(t),B_2(t),B_3(t)\big)^\top,$$

and

$$A=\begin{pmatrix}-a_{11} & -a_{12} & -a_{13}\\ a_{21} & 0 & 0\\ a_{31} & a_{32} & -a_{32}\end{pmatrix}.$$

Following Roozen [43], the density function $\Phi(V)=\Phi(v_1,v_2,v_3)$ of the quasi-stationary distribution for model (3.12) near the origin satisfies the three-dimensional Fokker-Planck equation

$$\begin{aligned}-\sum_{i=1}^{3}\frac{\sigma_i^2}{2}\frac{\partial^2\Phi}{\partial v_i^2}+\frac{\partial}{\partial v_1}[(-a_{11}v_1-a_{12}v_2-a_{13}v_3)\Phi]\\ +\frac{\partial}{\partial v_2}[a_{21}v_1\Phi]+\frac{\partial}{\partial v_3}[(a_{31}v_1+a_{32}v_2-a_{32}v_3)\Phi]=0.\end{aligned}$$

Since $G=\mathrm{diag}(\sigma_1,\sigma_2,\sigma_3)$ is a constant matrix, this solution of the above Fokker-Planck equation can be approximated by a Gaussian distribution

$$\Phi(V)=\bar{C}\exp\left\{-\frac{1}{2}(V-V^*)Q(V-V^*)^\top\right\},$$

where $V^*=(0,0,0)$, and Q is a real symmetric matrix, which is described by $QG^2Q+A^\top Q+QA=0$. If Q is positive definite, let $Q^{-1}=\Sigma$, then

$$G^2+A\Sigma+\Sigma A^\top=0. \tag{B.1}$$

According to the finite independent superposition principle [49], Eq. (B.1) can be replaced by the sum of the following three equations:

$$G_i^2+A\Sigma_i+\Sigma_i A^\top=0,\quad i=1,2,3,$$

where

$$\begin{aligned}&G_1=\mathrm{diag}(\sigma_1,0,0),\quad G_2=\mathrm{diag}(0,\sigma_2,0),\quad G_3=\mathrm{diag}(0,0,\sigma_3),\\&\Sigma=\Sigma_1+\Sigma_2+\Sigma_3,\qquad G^2=G_1^2+G_2^2+G_3^2.\end{aligned}$$

In order to verify the positive definiteness of Σ, we consider the corresponding characteristic equation of A as follows:

$$\varphi_A(\xi)=\xi^3+a_1\xi^2+a_2\xi+a_3, \tag{B.2}$$

where

$$\begin{aligned}&a_1=a_{11}+a_{32}>0,\\&a_2=a_{11}a_{32}+a_{12}a_{21}+a_{13}a_{31}>0,\\&a_3=a_{21}a_{32}(a_{12}+a_{13})>0.\end{aligned}$$

Furthermore, we can verify that $a_1a_2-a_3>0$. From now on, we will show the positive definiteness of Σ ($\Sigma=\Sigma_1+\Sigma_2+\Sigma_3$) by the following three steps.

Step 1. The algebraic equation is as follows:

$$G_1^2+A\Sigma_1+\Sigma_1A^\top=0. \tag{B.3}$$

Let $A_1=J_1AJ_1^{-1}$, where

$$J_1=\begin{pmatrix}1&0&0\\0&0&1\\0&1&0\end{pmatrix}.$$

As a result, we obtain that

$$A_1=\begin{pmatrix}-a_{11}&-a_{13}&-a_{12}\\a_{31}&-a_{32}&a_{32}\\a_{21}&0&0\end{pmatrix}.$$

Taking $B_1 = I_1 A_1 I_1^{-1}$, where

$$I_1 = \begin{pmatrix} 1 & 0 & 0 \\ 0 & 1 & 0 \\ 0 & -\dfrac{a_{21}}{a_{31}} & 1 \end{pmatrix},$$

we have

$$B_1 = \begin{pmatrix} -a_{11} & -\dfrac{a_{12}a_{21}+a_{13}a_{31}}{a_{31}} & -a_{12} \\ a_{31} & \dfrac{a_{32}(a_{21}-a_{31})}{a_{31}} & a_{32} \\ 0 & w_1 & -\dfrac{a_{21}a_{32}}{a_{31}} \end{pmatrix},$$

where

$$w_1 = -\frac{a_{21}a_{32}(a_{21}-a_{31})}{a_{31}^2}.$$

In the light of the value of w_1, we discuss them in the following two cases.

Case 1.1. When $w_1 \neq 0$, we can find the standard transformation matrix M_{11} such that $C_{11} = M_{11} B_1 M_{11}^{-1}$, where

$$M_{11} = \begin{pmatrix} -\dfrac{a_{21}a_{32}(a_{21}-a_{31})}{a_{31}} & \dfrac{a_{21}a_{32}^2(a_{21}-a_{31})}{a_{31}^2} & \dfrac{a_{32}^2 a_{21}}{a_{31}} \\ 0 & -\dfrac{a_{21}a_{32}(a_{21}-a_{31})}{a_{31}^2} & -\dfrac{a_{21}a_{32}}{a_{31}} \\ 0 & 0 & 1 \end{pmatrix},$$

then we have that

$$C_{11} = \begin{pmatrix} -a_1 & -a_2 & -a_3 \\ 1 & 0 & 0 \\ 0 & 1 & 0 \end{pmatrix}.$$

Hence, C_{11} is a standard R_1 matrix.

At the same time, Eq. (B.3) can be transformed into the following form:

$$\begin{aligned} &(M_{11}I_1J_1)G_1^2(M_{11}I_1J_1)^\top + \big((M_{11}I_1J_1)A(M_{11}I_1J_1)^{-1}\big)(M_{11}I_1J_1)\Sigma_1(M_{11}I_1J_1)^\top \\ &\quad + (M_{11}I_1J_1)\Sigma_1(M_{11}I_1J_1)^\top \big((M_{11}I_1J_1)A(M_{11}I_1J_1)^{-1}\big)^\top = 0, \end{aligned}$$

which is $G_0^2 + C_{11}\Sigma_0 + \Sigma_0 C_{11}^\top = 0$, where

$$\Sigma_0 = \frac{1}{\rho_{11}^2}(M_{11}I_1J_1)\Sigma_1(M_{11}I_1J_1)^\top, \quad \rho_{11} = -\frac{a_{21}a_{32}(a_{21}-a_{31})\sigma_1}{a_{31}}.$$

Lemma A.3 reveals that Σ_0 is positive definite. Furthermore, one know that the specific form of positive definite matrix Σ_0 is

$$\Sigma_0 = \begin{pmatrix} \frac{a_2}{2(a_1a_2-a_3)} & 0 & -\frac{1}{2(a_1a_2-a_3)} \\ 0 & \frac{1}{2(a_1a_2-a_3)} & 0 \\ -\frac{1}{2(a_1a_2-a_3)} & 0 & \frac{a_1}{2a_3(a_1a_2-a_3)} \end{pmatrix}.$$

Therefore, we conclude that

$$\Sigma_1 = \rho_{11}^2 (M_{11}I_1J_1)^{-1}\Sigma_0\big((M_{11}I_1J_1)^{-1}\big)^\top$$

is positive definite.

Case 1.2. When $w_1 = 0$, there exists a new standard transformed matrix M_{12} such that $C_{12} = M_{12}B_1M_{12}^{-1}$, where

$$M_{12} = \begin{pmatrix} a_{31} & 0 & 0 \\ 0 & 1 & 1 \\ 0 & 0 & 1 \end{pmatrix}.$$

As a result,

$$C_{12} = \begin{pmatrix} -b_1 & -b_2 & -b_3 \\ 1 & 0 & 0 \\ 0 & 0 & -a_{32} \end{pmatrix}.$$

Because C_{12} and A are similar matrices, through the similarity invariant of the characteristic polynomial, one have

$$\varphi_A(\xi) = \varphi_{C_{12}}(\xi) = \xi^3 + (b_1 + a_{32})\xi^2 + (b_2 + a_{32}b_1)\xi + b_2a_{32}. \tag{B.4}$$

Comparing the coefficients of Eqs. (B.2) and (B.4), one get

$$\begin{aligned} &b_1 = a_1 - a_{32} = a_{11} > 0, \\ &b_2 = a_2 - b_1a_{32} = a_{12}a_{21} + a_{13}a_{31} > 0. \end{aligned}$$

Then the conditions of Lemma A.4 are satisfied. Hence, C_{12} is a standard R_2 matrix.

At the same time, Eq. (B.3) can be transformed into the following form:

$$\begin{aligned} &(M_{12}I_1J_1)G_1^2(M_{12}I_1J_1)^\top + \big((M_{12}I_1J_1)A(M_{12}I_1J_1)^{-1}\big)(M_{12}I_1J_1)\Sigma_1(M_{12}I_1J_1)^\top \\ &\quad + (M_{12}I_1J_1)\Sigma_1(M_{12}I_1J_1)^\top\big((M_{12}I_1J_1)A(M_{12}I_1J_1)^{-1}\big)^\top = 0, \end{aligned}$$

which is $G_0^2 + C_{12}\Theta_0 + \Theta_0C_{12}^\top = 0$, where

$$\Theta_0 = \frac{1}{\rho_{12}^2}(M_{12}I_1J_1)\Sigma_1(M_{12}I_1J_1)^\top, \quad \rho_{12} = a_{31}\sigma_1.$$

Lemma A.4 reveals that Θ_0 is positive semidefinite. Furthermore, one know that the specific form of positive semidefinite matrix Θ_0 is

$$\Theta_0 = \begin{pmatrix} \frac{1}{2b_1} & 0 & 0 \\ 0 & \frac{1}{2b_1 b_2} & 0 \\ 0 & 0 & 0 \end{pmatrix}.$$

Therefore, we conclude that $\Sigma_1 = \rho_{12}^2 (M_{12} I_1 J_1)^{-1} \Theta_0 ((M_{12} I_1 J_1)^{-1})^\top$ is positive semidefinite.

Step 2. The algebraic equation is as follows:

$$G_2^2 + A\Sigma_2 + \Sigma_2 A^\top = 0. \tag{B.5}$$

Similarly, let $A_2 = J_2 A J_2^{-1}$, where

$$J_2 = \begin{pmatrix} 0 & 1 & 0 \\ 0 & 0 & 1 \\ 1 & 0 & 0 \end{pmatrix}.$$

As a result, we obtain that

$$A_2 = \begin{pmatrix} 0 & 0 & a_{21} \\ a_{32} & -a_{32} & a_{31} \\ -a_{12} & -a_{13} & -a_{11} \end{pmatrix}.$$

Taking $B_2 = I_2 A_2 I_2^{-1}$, where

$$I_2 = \begin{pmatrix} 1 & 0 & 0 \\ 0 & 1 & 0 \\ 0 & \frac{a_{12}}{a_{32}} & 1 \end{pmatrix},$$

we have

$$B_2 = \begin{pmatrix} 0 & -\frac{a_{21} a_{12}}{a_{32}} & a_{21} \\ a_{32} & -\frac{a_{12} a_{31} + a_{32}^2}{a_{32}} & a_{31} \\ 0 & w_2 & -\frac{a_{11} a_{32} - a_{12} a_{31}}{a_{32}} \end{pmatrix},$$

where

$$w_2 = \frac{a_{11} a_{12} a_{32} - a_{12}^2 a_{31} - a_{12} a_{32}^2 - a_{13} a_{32}^2}{a_{32}^2}.$$

In the light of the value of w_2, we discuss them in the following two cases.

Case 2.1. When $w_2 \neq 0$, we can find the standard transformation matrix M_{21} such that $C_{21} = M_{21} B_2 M_{21}^{-1}$, where

$$M_{21} = \begin{pmatrix} a_{32}w_2 & -\dfrac{w_2(a_{12}^2 a_{31} + 2a_{12}a_{32}^2 + a_{13}a_{32}^2 + a_{32}^2 w_2)}{a_{32}a_{12}} & \dfrac{a_{11}^2 a_{32} - a_{11}a_{12}a_{31} - a_{12}a_{31}a_{32} - a_{13}a_{31}a_{32}}{a_{32}} \\ 0 & w_2 & -\dfrac{a_{32}(a_{12}+a_{13}+w_2)}{a_{12}} \\ 0 & 0 & 1 \end{pmatrix}.$$

Then we have that $C_{21} = C_{11}$. Thus, C_{21} is also a standard R_1 matrix.

At the same time, Eq. (B.5) can be transformed into the following form:

$$\begin{aligned}&(M_{21}I_2J_2)G_2^2(M_{21}I_2J_2)^\top + \big((M_{21}I_2J_2)A(M_{21}I_2J_2)^{-1}\big)(M_{21}I_2J_2)\Sigma_2(M_{21}I_2J_2)^\top \\ &\quad + (M_{21}I_2J_2)\Sigma_2(M_{21}I_2J_2)^\top \big((M_{21}I_2J_2)A(M_{21}I_2J_2)^{-1}\big)^\top = 0,\end{aligned}$$

which is $G_0^2 + C_{21}\Sigma_0 + \Sigma_0 C_{21}^\top = 0$, where

$$\Sigma_0 = \frac{1}{\rho_{21}^2}(M_{21}I_2J_2)\Sigma_2(M_{21}I_2J_2)^\top, \quad \rho_{21} = a_{32}w_2\sigma_2.$$

Therefore, we conclude that $\Sigma_2 = \rho_{21}^2(M_{21}I_2J_2)^{-1}\Sigma_0((M_{21}I_2J_2)^{-1})^\top$ is positive definite.

Case 2.2. When $w_2 = 0$, there exists a new standard transformed matrix M_{22} such that $C_{22} = M_{22}B_2M_{22}^{-1}$, where

$$M_{22} = \begin{pmatrix} a_{32}^2 & -a_{12}a_{31} - a_{32}^2 & a_{32}a_{31} \\ 0 & a_{32} & 0 \\ 0 & 0 & 1 \end{pmatrix}.$$

As a result,

$$C_{22} = \begin{pmatrix} -\bar{b}_1 & -\bar{b}_2 & -\bar{b}_3 \\ 1 & 0 & 0 \\ 0 & 0 & -\dfrac{a_{32}(a_{12}+a_{13})}{a_{12}} \end{pmatrix}.$$

Because C_{22} and A are similar matrices, through the similarity invariant of the characteristic polynomial, one have

$$\begin{aligned}\varphi_A(\xi) = \varphi_{C_{22}}(\xi) = \xi^3 + \left(\bar{b}_1 + \frac{a_{12}a_{32} + a_{13}a_{32}}{a_{12}}\right)\xi^2 + \left(\bar{b}_2 + \frac{\bar{b}_1(a_{12}a_{32} + a_{13}a_{32})}{a_{12}}\right)\xi \\ + \frac{\bar{b}_2(a_{12}a_{32} + a_{13}a_{32})}{a_{12}}.\end{aligned} \tag{B.6}$$

Comparing the coefficients of Eqs. (B.2) and (B.6), one get

$$\bar{b}_1 = a_1 - \frac{a_{12}a_{32} + a_{13}a_{32}}{a_{12}} = \frac{a_{12}a_{31} + a_{32}^2}{a_{32}} > 0,$$

$$\bar{b}_2 = a_2 - \frac{\bar{b}_1(a_{12}a_{32}+a_{13}a_{32})}{a_{12}} = a_{12}a_{21} > 0.$$

Then the conditions of Lemma A.4 are satisfied. Hence, C_{22} is a standard R_2 matrix.

At the same time, Eq. (B.5) can be transformed into the following form:

$$\begin{aligned}&(M_{22}I_2J_2)G_2^2(M_{22}I_2J_2)^\top + \big((M_{22}I_2J_2)A(M_{22}I_2J_2)^{-1}\big)(M_{22}I_2J_2)\Sigma_2(M_{22}I_2J_2)^\top\\ &\quad + (M_{22}I_2J_2)\Sigma_2(M_{22}I_2J_2)^\top\big((M_{22}I_2J_2)A(M_{22}I_2J_2)^{-1}\big)^\top = 0,\end{aligned}$$

which is $G_0^2 + C_{22}\bar{\Theta}_0 + \bar{\Theta}_0 C_{22}^\top = 0$, where

$$\bar{\Theta}_0 = \frac{1}{\rho_{22}^2}(M_{22}I_2J_2)\Sigma_2(M_{22}I_2J_2)^\top, \quad \rho_{22} = a_{32}^2\sigma_2.$$

Lemma A.4 reveals that $\bar{\Theta}_0$ is positive semidefinite. Furthermore, one know that the specific form of positive semidefinite matrix $\bar{\Theta}_0$ is

$$\bar{\Theta}_0 = \begin{pmatrix} \dfrac{1}{2\bar{b}_1} & 0 & 0 \\ 0 & \dfrac{1}{2\bar{b}_1\bar{b}_2} & 0 \\ 0 & 0 & 0 \end{pmatrix}.$$

Therefore, we conclude that $\Sigma_2 = \rho_{22}^2(M_{22}I_2J_2)^{-1}\bar{\Theta}_0((M_{22}I_2J_2)^{-1})^\top$ is positive semidefinite.

Step 3. Consider the algebraic equation

$$G_3^2 + A\Sigma_3 + \Sigma_3 A^\top = 0. \tag{B.7}$$

Let $A_3 = J_3 A J_3^{-1}$, where

$$J_3 = \begin{pmatrix} 0 & 0 & 1 \\ 1 & 0 & 0 \\ 0 & 1 & 0 \end{pmatrix}.$$

As a result,

$$A_3 = \begin{pmatrix} -a_{32} & a_{31} & a_{32} \\ -a_{13} & -a_{11} & -a_{12} \\ 0 & a_{21} & 0 \end{pmatrix}.$$

Denote the following standard transform matrix:

$$M_3 = \begin{pmatrix} -a_{13}a_{21} & -a_{11}a_{21} & -a_{12}a_{21} \\ 0 & a_{21} & 0 \\ 0 & 0 & 1 \end{pmatrix}.$$

Letting $C_3 = M_3 A_3 M_3^{-1}$, we obtain that $C_3 = C_{11}$. Thus, C_3 is also a standard R_1 matrix.

At the same time, Eq. (B.7) can be transformed into the following form:

$$\begin{aligned}&(M_3J_3)G_3^2(M_3J_3)^\top+(M_3J_3)A(M_3J_3)^{-1}(M_3J_3)\Sigma_3(M_3J_3)^\top\\&+(M_3J_3)\Sigma_3(M_3J_3)^\top\big((M_3J_3)A(M_3J_3)^{-1}\big)^\top=0,\end{aligned}$$

which is $G_0^2+C_3\Sigma_0+\Sigma_0C_3^\top=0$, where

$$\Sigma_0=\frac{1}{\rho_3^2}(M_3J_3)\Sigma_3(M_3J_3)^\top,\quad \rho_3=-a_{13}a_{21}\sigma_3.$$

As shown in **Step 1**, Σ_0 is a positive definite matrix. Therefore,

$$\Sigma_3=\rho_3^2(M_3J_3)^{-1}\Sigma_0\big((M_3J_3)^{-1}\big)^\top$$

is positive definite.

To sum up, if

$$\widehat{\mathcal{R}}_{c1}=\frac{p(1-\epsilon)\beta_1\lambda}{\big(k+\sigma_1^2/2\big)\big(k+\epsilon\gamma+\sigma_2^2/2\big)}>1$$

and $\overline{\mathcal{R}}_{c1}>\overline{\mathcal{R}}_{c2}$ hold, Σ_1 and Σ_2 are at least positive semidefinite, Σ_3 is positive definite. Hence, we conclude that $\Sigma=(\varpi)_{3\times3}=\Sigma_1+\Sigma_2+\Sigma_3$ is positive definite. Thus, there exists a local density function

$$\Phi(v_1,v_2,v_3)=(2\pi)^{-\frac{3}{2}}|\Sigma|^{-\frac{1}{2}}e^{-\frac{1}{2}(v_1,v_2,v_3)\Sigma^{-1}(v_1,v_2,v_3)^\top}$$

near the quasi-steady equilibrium $\overline{P}_1$. This completes the proof. □

Acknowledgments

The authors would like to thank the anonymous referees for very helpful suggestions and comments which led to improvements of our original manuscript.

Y. Tan, Y. Cai and W. Wang were supported by the National Natural Science Foundation of China (Grant Nos. 12071173, 12171192) and by the Huaian Key Laboratory for Infectious Diseases Control and Prevention, China (Grant No. HAP201704). S. Liu was supported by the National Natural Science Foundation of China (Grant No. 12301627). X. Sun was supported by the National Natural Science Foundation of China (Grant No. 12071366). Z. Peng was supported by the National Natural Science Foundation of China (Grant Nos. 82320108018, 82073673).

References

[1] A. M. Anderson et al., *Prevalence and correlates of persistent HIV-1 RNA in cerebrospinal fluid during antiretroviral therapy*, J. Infect. Dis., 215:105–113, 2017.

[2] E. L. Asahchop et al., *Reduced antiretroviral drug efficacy and concentration in HIV-infected microglia contributes to viral persistence in brain*, Retrovirology, 14(1):47, 2017.

[3] F. A. C. Azevedo et al., *Equal numbers of neuronal and nonneuronal cells make the human brain an isometrically scaled-up primate brain*, J. Comp. Neurol., 513(5):532–541, 2009.

[4] T. Babas et al., *Role of microglial cells in selective replication of simian immunodeficiency virus genotypes in the brain*, J. Virol., 77(1):208–216, 2003.

[5] N. Bachmann, *Determinants of HIV-1 reservoir size and long-term dynamics during suppressive ART*, Nat. Commun., 10(1):3193, 2019.

[6] C. T. Barker, F. Wang, and N. K. Vaidya, *Modeling antiretrovial treatment to mitigate HIV in the brain: Impact of the blood-brain barrier*, Bull. Math. Biol., 85(11):105, 2023.

[7] T. H. Burdo, A. Lackner, and K. C. Williams, *Monocyte/macrophages and their role in HIV neuropathogenesis*, Immunol. Rev., 254(1):102–113, 2013.

[8] J. Cai et al., *Evaluating the long-term effects of combination antiretroviral therapy of HIV infection: A modeling study*, J. Math. Biol., 90(4):36, 2025.

[9] Y. Cai et al., *The fluctuation impact of human mobility on the influenza transmission*, J. Frankl. Inst., 357(13):8899–8924, 2020.

[10] P. Castellano, L. Prevedel, and E. A. Eugenin, *HIV-infected macrophages and microglia that survive acute infection become viral reservoirs by a mechanism involving Bim*, Sci. Rep., 7(1):12866, 2017.

[11] M. Chinnadurai, M. E. Fatini, and A. Rathinasamy, *Stochastic perturbation to 2-LTR dynamical model in HIV infected patients*, Math. Comput. Simulation, 204:473–497, 2023.

[12] D. B. Clifford and B. M. Ances, *HIV-associated neurocognitive disorder*, Lancet Infect. Dis., 13(11):976–986, 2013.

[13] J. M. Conway and D. Coombs, *A stochastic model of latently infected cell reactivation and viral blip generation in treated HIV patients*, PLoS Comput. Biol., 7(4):e1002033, 2011.

[14] J. M. Conway and A. S. Perelson, *Post-treatment control of HIV infection*, Proc. Natl. Acad. Sci. USA, 112(17):5467–5472, 2015.

[15] V. Dahl et al., *Low levels of HIV-1 rna detected in the cerebrospinal fluid after up to 10 years of suppressive therapy are associated with local immune activation*, AIDS, 28(15):2251–2258, 2014.

[16] N. Dalal, D. Greenhalgh, and X. Mao, *A stochastic model for internal HIV dynamics*, J. Math. Anal. Appl., 341(2):1084–1101, 2008.

[17] I. D'orso and C. V. Forst, *Mathematical models of HIV-1 dynamics, transcription, and latency*, Viruses, 15(10):2119, 2023.

[18] C. Dufour, P. Gantner, R. Fromentin, and N. Chomont, *The multifaceted nature of HIV latency*, J. Clin. Invest., 130(7):3381–3390, 2020.

[19] E. Eisele and R. F. Siliciano, *Redefining the viral reservoirs that prevent HIV-1 eradication*, Immunity, 37(3):377–388, 2012.

[20] L. Gama et al., *Reactivation of simian immunodeficiency virus reservoirs in the brain of virally suppressed macaques*, AIDS, 31(1):5–14, 2017.

[21] C. Gavegnano and R. F. Schinazi, *Antiretroviral therapy in macrophages: Implication for HIV eradication*, Antivir. Chem. Chemother., 20(2):63–78, 2009.

[22] B. B. Gelman et al., *Neurovirological correlation with HIV-associated neurocognitive disorders and encephalitis in a HAART-era cohort*, J. Acquir. Immune Defic. Syndr., 62(5):487–495, 2013.

[23] S. Gianella et al., *Compartmentalized HIV rebound in the central nervous system after interruption of antiretroviral therapy*, Virus Evol., 2(2):vew020, 2016.
[24] D. R. Graham et al., *Initiation of HAART during acute simian immunodeficiency virus infection rapidly controls virus replication in the CNS by enhancing immune activity and preserving protective immune responses*, J. Neurovirol., 17:120–130, 2011.
[25] M. Han et al., *HIV-1 cell-to-cell spread overcomes the virus entry block of non-macrophage-tropic strains in macrophages*, PLoS Pathog., 18(5):e1010335, 2022.
[26] M. Harkess et al., *HIV transactivation: Stochastic modeling for studying the effects of BET inhibitors on the modulation of P-TEFb levels*, J. Theor. Biol., 599:112011, 2025.
[27] A. Hening et al., *Long-term behavior of stochastic SIQRS epidemic models*, J. Theor. Biol., 90(4):41, 2025.
[28] S. Iwami et al., *Cell-to-cell infection by HIV contributes over half of virus infection*, eLife, 4:e08150, 2015.
[29] L. D. Jones, J. W. Jackson, and S. B. Maggirwar, *Modeling HIV-1 induced neuroinflammation in mice: Role of platelets in mediating blood-brain barrier dysfunction*, PLoS One, 11(3):e0151702, 2016.
[30] I. Karatzas and S. E. Shreve, *Brownian Motion and Stochastic Calculus*, in: Graduate Texts in Mathematics, Vol. 113, Springer-Verlag, 1998.
[31] R. Khasminskii, *Stochastic Stability of Differential Equations*, in: Stochastic Modelling and Applied Probability, Vol. 66, Springer, 2011.
[32] D. L. Kolson, *Developments in neuroprotection for HIV-associated neurocognitive disorders (HAND)*, Curr. HIV/AIDS Rep., 19(5):344–357, 2022.
[33] R. León-Rivera et al., *Central nervous system (CNS) viral seeding by mature monocytes and potential therapies to reduce CNS viral reservoirs in the cART era*, mBio, 12(2):e03633-20, 2021.
[34] G. N. Llewellyn et al., *HIV-1 infection of microglial cells in a reconstituted humanized mouse model and identification of compounds that selectively reverse HIV latency*, J. Neurovirol., 24(2):192–203, 2017.
[35] X. Mao, *Stochastic Differential Equations and Applications*, Woodhead Publishing Limited, 2007.
[36] C. Marban et al., *Targeting the brain reservoirs: Toward an HIV cure*, Front. Immunol., 7:397, 2016.
[37] E. Merlini et al., *Inflammation and microbial translocation measured prior to combination antiretroviral therapy (cART) and long-term probability of clinical progression in people living with HIV*, BMC Infect. Dis., 21(1):557, 2021.
[38] R. W. Price and S. Spudich, *Antiretroviral therapy and central nervous system HIV type 1 infection*, J. Infect. Dis., 197(s3):S294–S306, 2008.
[39] K. Qi and D. Jiang, *The impact of virus carrier screening and actively seeking treatment on dynamical behavior of a stochastic HIV/AIDS infection model*, Appl. Math. Model., 85:378–404, 2020.
[40] W. C. Roda et al., *Modeling brain lentiviral infections during antiretroviral therapy in AIDS*, J. Neurovirol., 23(4):577–586, 2017.
[41] W. C. Roda, S. Liu, C. Power, and M. Y. Li, *Modeling the effects of latency reversing drugs during HIV-1 and SIV brain infection with implications for the shock and kill strategy*, Bull. Math. Biol., 83(4):39, 2021.
[42] L. Rong and A. S. Perelson, *Modeling latently infected cell activation: Viral and latent reservoir persistence, and viral blips in HIV-infected patients on potent therapy*, PLoS Comput. Biol., 5(10):e1000533, 2009.
[43] H. Roozen, *An asymptotic solution to a two-dimensional exit problem arising in population dynam-*

ics, SIAM J. Appl. Math., 49(6):1793–1810, 1989.
[44] S. Saeb et al., *Targeting and eradicating latent CNS reservoirs of HIV-1: Original strategies and new models*, Biochem. Pharmacol., 214:115679, 2023.
[45] Z. Shi and D. Jiang, *Environmental variability in a stochastic HIV infection model*, Commun. Nonlinear Sci. Numer. Simul., 120:107201, 2023.
[46] Z. Shi and D. Jiang, *A viral co-infection model with general infection rate in deterministic and stochastic environments*, Commun. Nonlinear Sci. Numer. Simul., 126:107436, 2023.
[47] N. Sun-Suslow et al., *The clinical utility of three frailty measures in identifying HIV-associated neurocognitive disorders: A cross-sectional comparison of the Fried Phenotype, Rockwood Frailty Index, and Veterans Aging Cohort Study Index*, Lancet Healthy Longev., 3:S3, 2022.
[48] Y. Tan et al., *A stochastic SICA model for HIV/AIDS transmission*, Chaos Soliton Fract., 165:112768, 2022.
[49] X. Tian and C. Ren, *Linear equations, superposition principle and complex exponential notation*, College Phys., 23(7):23–48, 2004. (In Chinese)
[50] C. Van Lint, S. Bouchat, and A. Marcello, *HIV-1 transcription and latency: An update*, Retrovirology, 10:67, 2013.
[51] C. Wallet et al., *Microglial cells: The main HIV-1 reservoir in the brain*, Front. Cell. Infect. Microbiol., 9:362, 2019.
[52] Y. Wang et al., *Global prevalence and burden of HIV-associated neurocognitive disorder*, Neurology, 95(19):e2610–e2621, 2020.
[53] Y. Wang, M. Lu, and D. Jiang, *Dynamic behavior of a general stochastic HIV model with virus-to-cell infection, cell-to-cell transmission, immune response and distributed delays*, J. Nonlinear Sci., 33(5):97, 2023.
[54] Y. Wang, K. Qi, and D. Jiang, *An HIV latent infection model with cell-to-cell transmission and stochastic perturbation*, Chaos Soliton Fract., 151:111215, 2021.
[55] Y. J. Yeh and Y. Ho, *Shock-and-kill versus block-and-lock: Targeting the fluctuating and heterogeneous HIV-1 gene expression*, Proc. Natl. Acad. Sci. USA, 118(16):e2103692118, 2021.
[56] Y. Yuan and L. J. S. Allen, *Stochastic models for virus and immune system dynamics*, Math. Biosci., 234(2):84–94, 2011.
[57] Y. Zhao and D. Jiang, *The threshold of a stochastic SIS epidemic model with vaccination*, Appl. Math. Comput., 243:718–727, 2014.
[58] B. Zhou, X. Zhang, and D. Jiang, *Dynamics and density function analysis of a stochastic SVI epidemic model with half saturated incidence rate*, Chaos Soliton Fract., 137:109865, 2020.
[59] M. C. Zink et al., *Simian immunodeficiency virus-infected macaques treated with highly active antiretroviral therapy have reduced central nervous system viral replication and inflammation but persistence of viral DNA*, J. Infect. Dis., 202(1):161–170, 2010.